Non-viral Gold Nanoparticle Mediated Delivery of CRISPR-Cas9 Ribonucleoprotein and Long DNA Transgenes into Primary Blood Cells

Rachel Cunningham

A dissertation

submitted in partial fulfillment of the

requirements for the degree of

Doctor of Philosophy

University of Washington

2025

Reading Committee:

Jennifer E. Adair, Chair

Justin Taylor

Aude Chapuis

Program Authorized to Offer Degree:

Molecular Medicine and Mechanisms of Disease

University of Washington

Abstract

Non-viral Gold Nanoparticle Mediated Delivery of CRISPR-Cas9 Ribonucleoprotein and Long DNA Transgenes into Primary Blood Cells

Rachel Cunningham

Chair of the Supervisory Committee:

Jennifer E. Adair

Department of Lab Medicine and Pathology

Gene editing using CRISPR systems has gained traction for its potential to treat various diseases. However, current gene editing therapies suffer from lack of affordable, scalable and synthetic delivery, especially for complex cargo such as the CRISPR ribonucleoprotein (RNP) complex and DNA templates required for insertion of specific genomic sequences. Development of an effective non-viral approach to RNP delivery could overcome these limitations and would be transformative for clinical translation and research. We previously reported a simple, synthetic gold-based nanoparticle which can deliver various CRISPR systems as RNP into primary hematopoietic stem and progenitor cells without the need for complex protein engineering (CRISPR-AuNP). Here, we describe a gold-based nanoparticle to simultaneously deliver CRISPR systems and large DNA templates which can encode transgenes (HDT-CRISPR-AuNP). HDT-CRISPR-AuNP can carry templates as long as ~2.1kb, with potential for larger cargo. We evaluated HDT-

CRISPR-AuNP for gene editing at two loci of interest with different transgenes. These nanoparticles were able to successfully engineer primary human T cells and hematopoietic stem and progenitor cells with insertion of an antigen-specific T-cell receptor (TCR) transgene. This proof-of-concept immune engineering study shows transgene integration and expression from various hematopoietic lineages and suggests a potential for efficacy in vivo.

Contents

Chapter 1: Introduction 1

Gene Therapy: Past to Present 1

CRISPR Systems for Gene Editing 4

CRISPR for Immune Engineering 7

Delivery Strategies 10

Chapter 2: Non-viral Delivery of CRISPR to Primary Blood Cells 16

Introduction: 16

Results: 17

Nanoparticle Synthesis and Characterization: 17

In vitro validation of CRISPR-AuNP Efficacy in Jurkat Cells: 23

CRISPR-AuNP Efficacy in Primary T Cells: 25

Nanoparticle-mediated Immune Engineering of Primary T and CD34+ Cells: 26

Discussion: 37

Conclusion: 39

Methods: 40

Materials: 40

Nanoparticle Synthesis: 40

Dynamic Light Scattering Characterization 44

Imaging by TEM 44

RNP Loading Characterization by SDS-PAGE 45

HDT Loading Characterization by Agarose Gel Electrophoresis 47

Jurkat Cell Culture 47

Primary T Cell Culture: 48

CD34+ Cell Culture 48

Cell Viability Measures 49

Confocal Microscopy 49

Flow Cytometry 50

gDNA Extraction and Sequencing 50

Confirmation of Template Insertion by PCR 51

Statistics and Data Reporting 51

Chapter 3: Discussion 52

Conclusions: 52

Future Directions: 54

Overall Conclusions: 58

Appendix: 59

Nanoformulation Optimization & In Vivo Studies 59

Acknowledgements 68

References 69

Chapter 1: Introduction

Gene Therapy: Past to Present

Gene therapies consist of treatments that modify the genomes of cells within the body for therapeutic downstream effect [1-3]. Through an array of different technologies, these therapies modify existing genes or introduce novel ones to correct for inborn defects or deleterious somatic mutations [2, 4, 5]. Modern gene therapies were conceptualized as early as the 1960s, but clinical trials were not started in human subjects until the early 1990s [6]. Initial studies had mixed results marked by success in curing a patient of her congenital immune deficiency [7], but also unexpected adverse events including the 1999 death of Jesse Gelsinger , a teenager enrolled in a clinical trial to cure an inborn metabolic disease. While enrolled in a gene therapy trial at the University of Pennsylvania, Gelsinger developed a fatal immune reaction to the modified adenovirus used to deliver the therapeutic transgene [8].

The catastrophic adverse event associated with the delivery vehicle for gene therapy in the Gelsinger case put a years-long damper on enthusiasm for gene therapy, with all five of the gene therapy clinical trials run through the University of Pennsylvania being halted as an immediate effect [9].

In the years to follow, children participating in clinical trials in Europe developed cancer after treatment, caused by the retroviral vector vehicles used to deliver gene therapy, which introduced genotoxic mutations in blood stem cells [10-12]. These outcomes were sufficient to dull the scientific community's interest in gene therapies for nearly a decade to come.
In the mid-1980's, new delivery vehicles in the forms of less immunogenic engineered adeno-

associated viral vectors (AAV) for exogenous delivery of double-stranded DNA (dsDNA) [13] and less mutagenic self-inactivating lentiviral vectors (LV) for endogenous integration of new transgenes [14, 15] promised the efficiency of viral delivery with improved safety. These two viral vector systems would later become the vehicles for the first authorized gene therapies in the U.S. in 2017 (AAV therapy voretigene neparvovec-rzyl (Luxturna™))[16, 17] and LV therapies tisagenlecleucel (Kymriah™)[18] and axicabtagene ciloleucel (Yescarta™) [19]. However, improved viral vectors were not solely responsible for jumpstarting gene therapy research after a long fallow period.

In the late 1990s, the development of novel methods of genome editing spurred renewed interest and investment in the field. Engineered zinc finger nuclease (ZFN) proteins capable of introducing sequence-directed double-stranded breaks (DSB) in genomic DNA entered the field in 1994 [20]. ZFNs are engineered restriction enzymes composed of a pair of three to six flanking zinc-finger motif DNA binding domains fused to central, dimerized DNA cleaving domains, usually from the endonuclease FokI [21]. While these represented an important advance in programmable endonuclease systems, the fact that the ZFN domain needs to be specially engineered to bind the desired cut site in the DNA made this system somewhat cumbersome [22, 23]. ZFNs are still of potential clinical use and have been subject to a few clinical trials, including for glioblastoma [24] and HIV [25]. Later advances in gene editing tools include transcription activator-like effector nucleases (TALENs) and meganucleases [22]. The former is similarly a fusion protein comprised of a several linked DNA recognition domains and a cutting domain [26]. The distinguishing factor separating TALENs from ZFNs is that the TALEN DNA binding domain recognizes only one nucleotide, whereas each zinc-finger domain must

bind three nucleotides at once [27]. This allows the design of TALENs to be much more modular in its site recognition and provides greater flexibility for cut site choice. Some in vitro studies have also found less cytotoxicity and higher on-target editing when comparing editing capabilities of ZFNs and TALENs [28, 29]. Meganucleases, meanwhile, are endonucleases based on naturally occurring homing nucleases that are encoded in the introns of mammalian DNA [30]. These endonucleases recognize DNA sequences of up to 40bp, lending high specificity as well as low cytotoxicity due to their mammalian nature [31]. Meganucleases can also be conjugated to TAL domains, allowing for highly-specific megaTALs with the recognition capacity of TALENs and specificity, feasibility, and immunogenicity of meganucleases [32]. These endonuclease systems generated significant excitement in the gene therapy field and set the stage for the most widely-used programmable nuclease in current use [33].

In 2012, a bacterial immune enzyme was found to be amenable to RNA-dependent reprogramming, the end result being an endonuclease that could be directed to create a double-stranded break (DSB) anywhere in the DNA [34, 35]. The ability to synthesize a custom RNA molecule is much faster than engineering a protein, the major limitation required for reprogramming ZFNs, meganucleases and TALENs [34]. The potential of such clustered regularly interspaced short palindromic repeats (CRISPR) associated (Cas) endonucleases to cut at a directed site revolutionized the field. Just 11 years later, the first CRISPR gene therapy (exagamglogene autotemcel (Casgevy®)), was authorized by the U.S. Food and Drug Administration [36].

CRISPR Systems for Gene Editing

CRISPR systems were discovered in the late 1980s and were independently characterized by several groups conducting basic research on various bacteria [37, 38]. CRISPR refers to sequences in bacterial DNA noted to be associated with Cas proteins, which formed ribonucleoprotein (RNP) complexes with the RNA sequences transcribed from these DNA sequences, hence the term CRISPR/Cas systems. Researchers found that many of the sequences encoded in CRISPR RNAs (crRNA) were found also in phage viruses that infect bacteria [38]. It was concluded that the CRISPR/Cas systems within bacteria function as immune systems, with Cas proteins using crRNAs in the bacterial genome to direct cutting activity towards invading viral DNA [39]. By producing the three parts of CRISPR RNP—the nuclease protein along with two RNA features, crRNA and the trans-activating crRNA (tracrRNA) that stabilizes the RNA-protein interaction—separately, the bacteria create a highly modular endonuclease capable of targeting specific DNA sequences for degradation [35]. Doudna et al. found that a particular Cas protein in *Streptococcus pyogenes*, Cas9, could be engineered to cut at any desired site within bacterial or mammalian DNA [35, 40], so long as that site included a protospacer-adjacent motif (PAM) sequence, a conserved 3-4 nucleotides adjacent to the cut site. The ease of use and relatively low cost of CRISPR systems caused an explosion in gene editing technology [34, 41, 42].

The development of a programmable nuclease promised new genetic engineering strategies for different disease indications. CRISPR-mediated gene editing begins with RNP entry into the nucleus using a suitable delivery method, most commonly electroporation. There RNP melts and binds the DNA to form an RNA-DNA hybrid. If there is a suitable PAM within the sequence,

the protein will bind that sequence and unwind the double-stranded DNA adjacent to determine alignment with the corresponding RNA guide element. If pairing is sufficient to hold the complex in place, another catalytic domain mediates cutting of both strands of DNA, resulting in blunt-ended or overhanging DSB in the DNA [43].

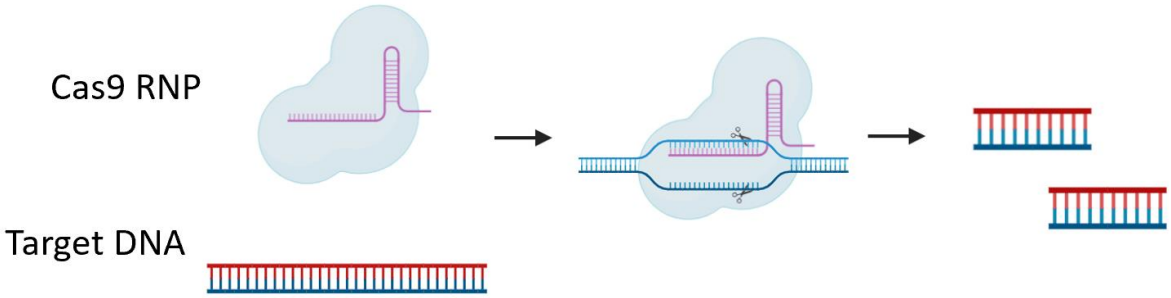

Figure 1. Cas9 RNP complex binds and cuts target DNA sequence. *Cas9 complex formed from Cas9 protein, gRNA, and tracrRNA hairpin is able to bind and melt DNA complementary to the gRNA. Both strands of DNA are cleaved at the cut site to generate a blunt-ended DSB. Diagram made with BioRender.*

After the formation of a DSB, the cell may utilize any of several endogenous DNA-repair mechanisms. The first and most frequent is non-homologous end-joining (NHEJ) wherein each end of the DSB is subject to degradation by exonucleases and endonuclease to form short regions of homology between the two DNA ends. The resulting overhangs allow re-ligation of the DNA, often with the formation of insertion or deletion mutations (indels) [44]. Alternately, the cell may engage in other DNA repair mechanisms, such as microhomology mediated repair (MMR) or homology-directed repair (HDR) [44-46]. Of these, HDR is considered clinically valuable for introduction of designer DNA sequences at the site of CRISPR activity. HDR involves

further resection of single strands from the site of the DSB. The sister chromatid is then recruited to serve as a template for resynthesizing the digested bases to create enough homology between the two DNA ends to ligate the cut, preserving genomic integrity of the locus, but removing heterozygosity [47].

The HDR pathway can be manipulated to integrate exogenous DNA into the host genome by co-delivering excess amounts of template DNA which can serve as a replacement sister chromatid during repair. These template DNAs encode a transgene flanked by sequences homologous to the cut site [48]. CRISPR-mediated transgene integration through HDR allows for expression of transgenes from their native loci, with little chance for off-target transgene integration as long as the cognate PAM and gRNA specificity are present at the desired locus [49]. Notably, the repair mechanism used depends on the proteins available to stabilize the free ends of the DSB, and is related to cell cycle phases [47].

To date, thousands of CRISPR systems have been identified, many with unique PAM, gRNA and nuclease activities [50-52]. Engineering of these systems to fuse RNA-guided genomic activity with alternative functionality such as base modification (i.e. base editing) [53], reverse transcription (i.e. prime editing) [54], and recombination such as eePASSIGE (eeBxb1Prime-Assisted Site-Specific Integrase Gene Editing)[55] or CAST (CRISPR-associated transposons) have further expanded utility [56]. CRISPR therapies transformed the methods by which desirable mutations could be made in the genome, epigenome, and mitochondrial DNA, and with that came more varied disease indications for gene therapy. The first CRISPR-based medicines approved by the FDA were designed to treat sickle cell disease and beta-thalassemia [36, 57], two common genetic conditions that result in malformation of hemoglobin and subsequent

drop in life quality and expectancy [58, 59]. At present there are more than 113 clinical trials of some type of CRISPR genome engineering in progress, with hundreds to thousands in pre-clinical development [1, 60, 61]. All of the current development is happening in countries defined as high- or upper-middle income by the World Bank [62].

It must be acknowledged, however, that the majority of the global disease burden is carried by low and middle income countries (LMICs) [63]. As the most expensive drugs in the world, gene therapies, CRISPR or virus-based, are out of reach for the global majority patients who require them [64]. Further, due to the cost of necessary research machinery such as electroporators, CRISPR research is difficult to conduct in the LMICs that stand to most benefit from them [65]. Genetic engineering efficacy and safety is dependent upon the patient genome and the human genome at large. The widest range of human genetic diversity is present on the African continent [66], which currently houses only a few research institutes and hospitals equipped to carry out CRISPR research, though emerging economies are expanding research investment [62]. Expanding access to local CRISPR-based research in LMICs is vital for global translation and transformative medicine. The disconnect between the potential efficacy of gene and cell therapies and the reality of their extremely limited accessibility—and therefore practical usage cases—represents a major reckoning for the field of gene therapy.

CRISPR for Immune Engineering

CRISPR technologies are of particular interest for their potential ability to mediate several kinds of genetic editing highly relevant to the specialty of immune engineering. These can include making genetic edits in differentiated immune cells or hematopoietic stem and progenitor cells (HSPC) that differentiate to form all blood cell lineages [67]. In some cases, CRISPR-mediated

DSBs targeted to specific loci can knock down expression of native protein while simultaneously allowing translation of transgenes integrated into the cut site [68, 69], a method that is useful for engineering T cell receptors (TCR) in particular. Introducing novel transgenic TCRs and in some cases CARs into the native TCR loci has shown significant promise in preclinical studies and several CRISPR-based T cell engineering technologies have made their way to clinical trials [70-72]. While many CAR-T therapies currently approved are engineered using lentiviral means [73], CRISPR editing may offer the possibility of simultaneously knocking down other genes of interest, such as checkpoint inhibitors like programmed cell death protein 1 (PD-1)or cytotoxic T lymphocyte-associated protein 4 (CTLA-4) [74]. Several such T cell therapies with multiplexed CRISPR engineering are currently in clinical trials [75-78].

CRISPR systems have also shown success in engineering antibody expression from B cells. A 2019 study by Moffett et al. found that when the necessary components are electroporated into cells ex vivo prior to implantation in mice, engineered B cells persist in the murine model and produce engineered antibody in response to pathogen challenge [79]. Another study by the Barzel group showed successful expression of anti-HIV broadly-neutralizing antibodies (bnAbs) after direct injection of dual AAV carrying transgenes coding for Cas9 and the bnAb respectively [80]. Other groups have shown similar success in using CRISPR to introduce novel antibody-coding genes into B cells and plasma cells [81-83].

Alternate target cell populations for immune engineering include natural killer (NK) and natural killer T cells (NKTs), which are of particular interest in the field of oncology for their ability to mediate cell-killing without requiring major histocompatibility complex (MHC) recognition [84]. CRISPR-mediated generation of cell products such as CAR-NK therapies that

result in non-MHC-restricted target-specific cell killing has been tested in animal models and in patients with multiple myeloma [85].

Engineering lymphoid cells to express engineered receptor proteins is valuable in the fields of immunology, oncology, and infectious disease research [86, 87]. As CAR-T therapies gain traction for treatment of cancer, there is significant interest in cutting the cost of producing these engineered cell products [88]. Tisagenlecleucel, (KYMRIAH™), the first FDA approved CAR-T drug, is manufactured in a 22-day long process using LV vector transduction and requiring highly specialized environments and equipment for its production [89]. Tisagenleucel carries a price tag of nearly half a million US dollars [88], preventing rollout in the developing world. Much of this cost is driven by the high titers of LV necessary for achieving significant cell engineering [90]. Streamlining or automating the manufacturing process in a decentralized approach and reducing the cost of generating genetically engineered T cells could have a major impact on access to cancer therapies, and some LMICs such as India are innovating in this space out of necessity [91]. Replacing LV with CRISPR engineering could play a role in making gene therapies more affordable and accessible.

Research is also being done on engineering HSPC rather than mature lymphoid progeny [92, 93]. Embedding transgenes coding for therapeutic TCRs or antibodies into their native loci in undifferentiated HSPC has been shown to result in production of the desired protein by daughter cells of the edited stem cell [94]. Some speculate that this system, which mimics endogenous immune function more closely than LV transduced lymphocytes, may have advantages in mediating an appropriate immune response [95]. Additionally, targeting HSPC for immune engineering may result in a lifelong reservoir of engineered cells derived from edited

stem cells rather than relying on the formation of memory T or B cells from engineered mature lymphocytes [94, 95]. However, major hurdles still exist in the field of HSPC engineering. The inherent “stemness”, or stem cell-like phenotypic characteristics, of these cells determine their ability to engraft into the bone marrow niche and carry out functions such as stem cell repopulation and differentiation into specialized lineages [96]. Even slight perturbations can affect stemness, damaging the HSPC ability to engraft in the desired space and their proliferative capacity [97]. The nature of the perturbation may have variable effects on stemness and overall cell fitness—some studies show that viral infection such as that used in LV and AAV systems may lower stemness over time [98]. Engineered HSPC are therefore typically tested for fitness using in vitro assays such as colony-forming unit (CFU) analysis and serial stem cell transplantation in murine models [99]. These assays can help insure that inserting novel transgenes into the HSPC genome does not deleteriously affect their ability to carry out stem cell function.

While many studies on HSPC engineering have primarily involved knocking out genes implicated in HIV infection, like CCR5 [100], others have shown successful expression of bnAb transgenes from blood cells derived from edited stem cells [101]. Such studies lay the groundwork for the generation of HSPC therapies that can result in lifelong immunity against target pathogens.

Delivery Strategies

The question of how to best deliver gene therapy is deeply intertwined with the editing technology itself. In terms of ex vivo cell engineering, or treatment of cells extracted from the

body for later implantation into a patient, delivery method and subsequent cell manipulation differs for viral versus non-viral therapy methods.

Viral therapies, whether LV or AAV, can be added directly into cell media where the virus will engage its target receptors on the cell to achieve entry [102] and then traffic to the nucleus to integrate its transgene payload into its preferred site in the cell genome [102, 103]. Ease of delivery and biologically evolved cellular trafficking gives viral therapies a distinct advantage over many non-viral delivery methods. However, both LV and AAV systems are limited by the capacity of the viral genome to carry long transgenes. LV can package between 8 and 10 kilobases (kb), which is sufficient for many immune engineering purposes [104]. AAV, however, can only carry up to 5kb, which may cause problems if the AAV is designed to carry a sequence coding for CRISPR protein and sgRNA in addition to a long transgene [105].

Non-viral therapies are largely comprised of CRISPR systems [1, 61]. CRISPR editing machinery can be delivered as DNA in the form of a plasmid, as mRNA, or as a fully formed RNP [106, 107]. Each has benefits and drawbacks, with DNA and mRNA delivery resulting in longer-term protein expression at the expense of more potential off-target activity [108]. Oligonucleotides can be delivered in vitro by electroporation or by conjugation to a chemical transfection reagent such as lipofectamine or polyethylenimine (PEI) [109]. Protein delivery is more complicated but may be more desirable when treating cells that have a slow rate of translation and would be delayed in expressing CRISPR from DNA or mRNA [110]. A more cogent consideration is the downstream effects of off-target CRISPR cutting in a cell—prolonged expression of RNP from nucleic acid may have more deleterious effects in stem cell populations than in mature, shorter-lived cells [107,

110]. RNP can also be delivered via electroporation and in some cases by transfection reagents, although not as efficiently as DNA or mRNA [106, 108].

For both viral and non-viral therapies, in vitro delivery requires traversing the biology of purified cells in controlled culture conditions, whereas in vivo delivery adds the complexity of physiologic environments and navigation of complex tissues to find target cells. In vivo gene therapy is a lofty goal, and one that has seen increased research in recent years [111]. Viral therapies are immunogenic, as seen in early clinical trials [8, 13]. The inherent immunogenicity of AAV means that no AAV of the same serotype can be administered twice to the same patient [112], which may limit dosing or limit therapy options for patients. In vivo delivery of AAV has been approved for treating genetic conditions of the eye and central nervous system, as well as liver for the treatment of hemophilia [113].

LV therapies are currently approved only for ex vivo use [114, 115]. Some early preclinical work suggests LV administration could be safe and effective in vivo, with porcine models of an inborn error of metabolism demonstrating almost complete abrogation of disease symptoms when treated with LV [116], but many studies show widespread pre-existing immunity to commonly used viral envelopes [112]. Further, some researchers have voiced concerns about the potential of off-target LV integration into the genome and the risk of false-positive HIV testing as a result of immune response to LV therapies [117].

Engineered virus-like particles (eVLPs) consist of a viral envelope engineered to package internal cargo without carrying a viral genome [118, 119]. While eVLPs have shown promise preclinically, they are still costly and complicated to produce and require additional protein engineering of

CRISPR cargo to mediate packaging. Since these delivery vehicles still utilize envelope glycoproteins from viruses, immunogenicity will still occur while false-positive virus tests results will not. All viral vectors and eVLP require a living cell system for assembly, which requires co-delivery of multiple “pieces” of the viral particle into cell lines, subsequent culture and collection of media during peak viral particle production, and then purification of collected viral particles from media components and cellular debris. This makes viral vector production complex, inefficient, lengthy, and costly [120].

In order to avoid the expense of viral synthesis and specialized manufacturing facilities, many researchers have turned to fully synthetic nanoparticles instead of viral or virus-like systems [121]. Polymeric nanoparticles (polyplexes), which package gene editing cargo in a shell or among a polyplex of positively charged polymer, are cheap and easy to formulate, as well as being highly tunable [122], but often have trouble packaging complex cargo like CRISPR RNP rather than mRNA [123]. To date, the most common cargo for polyplex formation and delivery is DNA, and primarily for cancer [124]. Notably, polymeric nanoparticles are often associated with significant toxicity in murine models and in human patients [125].

Lipid nanoparticles (LNP) consist of cationic lipids encapsulating various cargo [123]. These have garnered significant interest since the success of LNP mRNA vaccines [126], but similarly face difficulty when loading multiple types of cargo as in the case of CRISPR RNP and a DNA transgene [123]. Moreover, multiplexing CRISPR components in LNPs is currently quite difficult. While LNPs have been shown to successfully encapsulate both RNP and template DNA for HDR, these templates are necessarily short due to the difficulties of incorporating complex, long DNA into lipid formulations [127]. Lipid nanoparticles carrying CRISPR mRNA have been shown to

successfully treat transthyretin amyloidosis when administered to mice in vivo [128], but the utility of these for delivering long transgenes and RNP to HSPC is limited.

Nanoparticles that do not encapsulate cargo, but rather bind it to a central core, have become an area of interest in gene therapy [121]. Metal core nanoparticles such as iron oxide [129], titanium [130], or gold [131, 132], have been used in a number of clinical applications and show good tolerability when administered locally or systemically [121]. These particles can form stable and predictable chemical interactions between core surface atoms and various cargo atoms with covalent or non-covalent tethering. Cargo loading can also occur through electrostatic, hydrophobic and oxidative interactions [129-132]. The ability to visualize metal core nanoparticles with various electron microscopic techniques, and the ability to determine gold mass doses by inductively-coupled mass spectrometry permits accurate calculations of core surface area volumes, which when combined with known cargo sizes and structures creates scalable and predictable cargo loading. Metal core particles themselves are typically non-immunogenic and bioinert [133], making them attractive candidates for gene therapy nanoparticle formation. Gold core nanoparticles (AuNP) are of particular interest. Several groups have shown that chemical modification can enable gold core particles to bind CRISPR RNP [131, 132] for delivery intracellularly. AuNP are easy to synthesize in a variety of sizes [134] and can be conjugated to any number of molecules through a variety of interactions, in particular when molecules contain a free thiol group and any charge repulsions can be managed [131, 132].

The Adair lab showed in 2019 that AuNP can be formulated to carry Cas9 and Cas12a RNP along with short DNA transgenes, that these CRISPR-AuNP are taken up by primary human

hematopoietic cells in vitro and can mediate gene editing in HSPC [132]. The ability of CRISPR-AuNP to enter cells in culture requires the cells to be endo- or pinocytosing. Subsequent escape from these compartments after uptake is necessary for intracellular delivery and requires addition of cationic polymer (low molecular weight, branched chain PEI) to the cargo via electrostatic interactions. This platform is synthesizable on the benchtop in less than a day and can carry multiple types of CRISPR cargo [132]. However, subsequent optimization of the synthesis protocol was required to maximize active RNP loading for Cas9 systems, including modification of polymers to include polyethylene glycol and core-tethering thiol modifications [135]. This improved CRISPR-AuNP formulation is even simpler to synthesize in a shorter time with commercially available reagents and has potential for in vivo administration [135]. If CRISPR-AuNP could carry CRISPR RNP and long therapeutic transgenes, it would present a transformative impact on the field of immune engineering by simplifying delivery of this complex cargo to be passive, akin to viral-mediated delivery, but with a synthetic particle that can be manufactured quickly and without the need for living cell systems or protein engineering.

Chapter 2: Non-viral Delivery of CRISPR to Primary Blood Cells

Introduction:

An effective non-viral gene therapy nanoparticle must demonstrate the ability to carry CRISPR RNP or mRNA, and/or DNA. The most desirable form of delivery depends on the target tissue, its rate of transcription and translation, and the risks of off-target CRISPR cutting in the intended cell type. Hematopoietic stem and progenitor cells (HSPC) are of interest for their ability to generate daughter cells that also contain the desirable genetic edit. For HSPC, CRISPR RNP delivery is most desirable due to the slow translation rate of these quiescent cells and the increased risk of downstream genotoxicity resulting from off-target nuclease activity [110]. This poses a problem for current nanoparticle therapies, which are largely lipid based (lipid nanoparticle, LNPs) or polymer based (polyplexes), as these cationic molecules most efficiently encapsulate negatively charged oligonucleotides (DNA or mRNA) [123, 124]. Engineered virus-like particles, or eVLPs, have demonstrated excellent activity in HSPC and successfully encapsulate CRISPR RNP, however these have only been shown to deliver short DNA transgenes and must also be formulated using specially engineered CRISPR nucleases [118, 120].

We have previously demonstrated the efficacy of gold-core nanoparticles (AuNP) as CRISPR RNP and short (~80nt) ssDNA template delivery vehicles to primary human HSPC [132, 135]. This nanoparticle, CRISPR-AuNP, delivers Cas9 RNP alone and shows significant editing potential at the *β-2-microglobulin* locus (*B2M*) in cell lines and primary human blood cells. This nanoparticle is easily synthesized in under 6 hours using no highly specialized equipment, and costs ~$64 per 20ug dose, which is sufficient to treat $1x10^6$ cells. CRISPR-AuNP is taken up passively by cells in

culture where a PEI-PEG copolymer coating enables it to escape the endosome and enter the nucleus, where the cargo become unbound from the gold surface and engage in gene editing . This platform has shown efficacy in vitro in hematopoietic stem and progenitor cells (HSPC), and with multiple CRISPR systems, demonstrating strong modularity for further development and possibly in vivo potential. The goal of this study is to expand the cargo delivered by CRISPR-AuNP to include DNA. Here, we propose a gold-based non-viral nanoparticle capable of simultaneously packaging Cas9 RNP and long (2.1kb) double-stranded DNA (dsDNA) transgenes to serve as homology-directed repair templates (HDT). By conjugating large transgene-encoding HDT to this nanoparticle, we increase its potential to mediate different types of therapeutic edits in vitro and potentially in vivo.

Results:

Nanoparticle Synthesis and Characterization:

We first attempted to add a long, transgene encoding HDT to our 3rd generation CRISPR-AuNP via electrostatic forces (Figure 1A). A 2.1kb dsDNA HDT encoding an enhanced green fluorescent protein (GFP) transgene flanked by homology arms to the human *B2M* locus was synthesized by polymerase chain reaction (PCR) for testing (Table 1). We evaluated several titrations of HDT added to the CRISPR-AuNP after initial formulation and assessed particle characteristics by dynamic light scattering (DLS) to establish suitability for clinical use (Figure 1B). While each of the dsDNA titrations chosen resulted in acceptably sized nanoparticles (i.e. <200nm hydrodynamic diameter) [136] when analyzed via DLS, none demonstrated clinically-acceptable polydispersity index (PDI) values of less than 0.3 [136, 137] (Figure 1B). This suggests that AuNP

core surface charges remain unsatisfied, resulting in aggregation of particles to achieve stability. We previously demonstrated that binding of gRNA could satisfy AuNP core surface charges [132] in our 1st generation CRISPR-AUNP. We hypothesized that formation of an inner layer of HDT covering the AuNP surface would permit a polyplex layer to bind and form covalent linkages to the gold core, trapping any loose DNA in the polymer with charge left unsatisfied by RNP (Figure 1C).

To achieve HDT binding to the AuNP core surface, the 2.1kb dsDNA HDT encoding GFP for integration at *B2M* was PCR-synthesized using a forward primer that contained a 12-carbon oligoethylene glycol (OEG) spacer with a 5' terminal thiol. This 5'-SH-OEG-HDT was used to coat the gold core at different ratios of HDT molecules per individual AuNP. We found that while higher ratios of HDT to AuNP resulted in monostable particles, the hydrodynamic diameters of these particles exceeded 200nm, which is expected to compromise cellular entry [138] (Figure 1D).

Since the stabilizing gRNA in our 1st generation CRISPR-AuNP were short (~23nt), we tried stabilizing the AuNP surface with short SH-OEG-ssDNA (25nt), in addition 5'-SH-OEG-HDT (Figure 1E). This mixed DNA monolayering resulted in monostable nanoparticles with four HDT molecules and at least 200 ssDNA molecules per AuNP core (Figure 1F). The ratio of 4HDT:200ssDNA was chosen for further studies in order to maximize HDT loading.

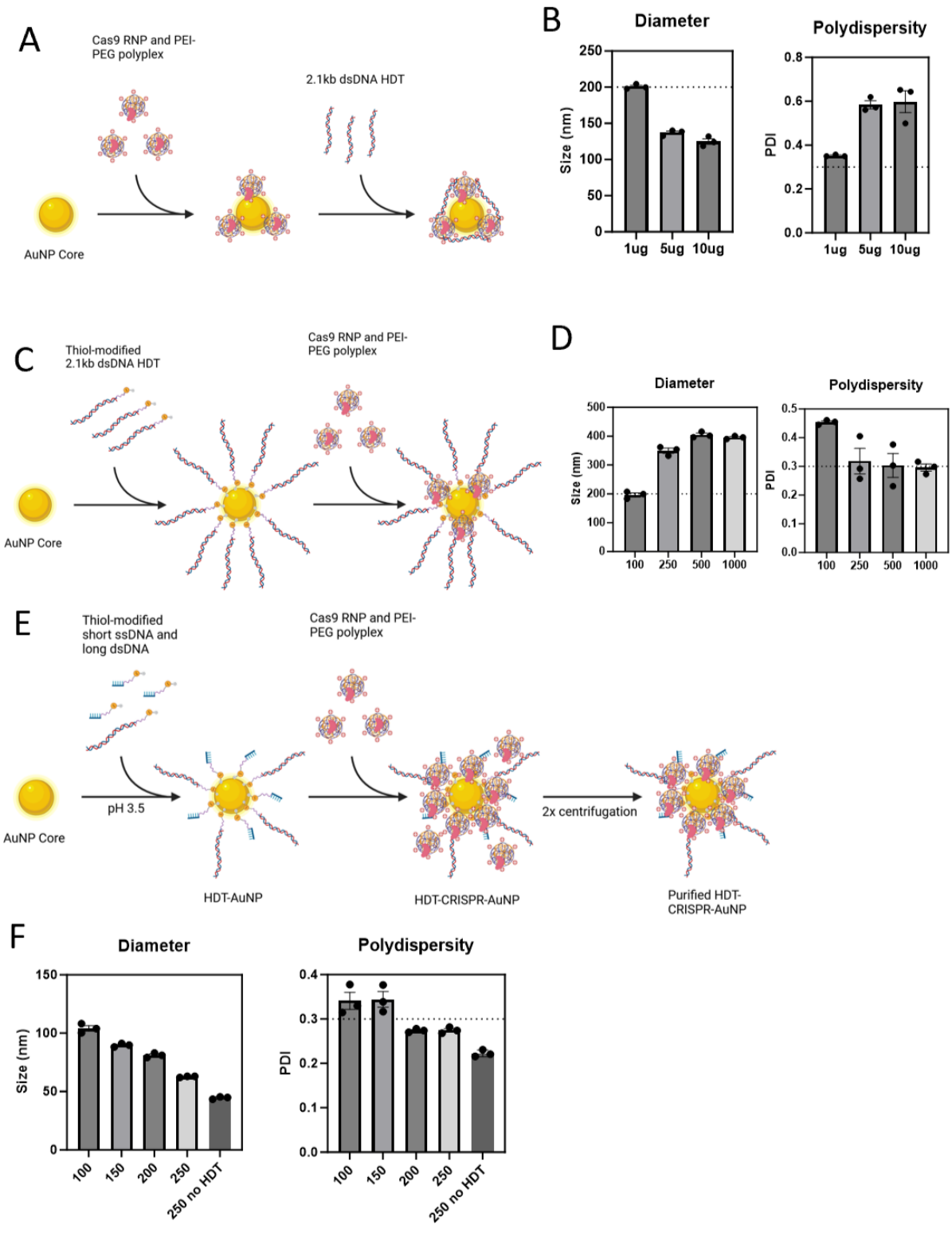

Figure 1. Successful addition of HDT cargo to CRISPR-AuNP requires stabilization of unsatisfied core surface charges prior to CRISPR-RNP polyplex loading. *(A) Schematic of initial HDT-CRISPR-*

AuNP synthesis by formulating CRISPR-AuNP and decorating the nanoparticle surface with electrostatically-bound HDT. (B) DLS analysis of hydrodynamic diameter (left) and polydispersity (PDI) (right). Data represent three technical replicates (dots) as means (gray bars) ± standard error of the mean (error bars). Horizontal dashed lines represent the upper acceptable limits for size and PDI. (C) Schematic of altered HDT-CRISPR-AuNP synthesis by first forming a layer of thiol-modified HDT around the AuNP surface and then adding CRISPR RNP polyplexes. (D) DLS analysis of hydrodynamic diameter (left) and PDI(right). Data represent three technical replicates (dots) as means (gray bars) ± standard error of the mean(error bars). Horizontal dashed lines represent the upper acceptable limits for size and PDI. (E) Schematic showing surface stabilization of AuNP by the addition of a short, thiol-modified ssDNA in addition to thiol-modified HDT, then followed by CRISPR-RNP polyplex addition. (F) DLS analysis of hydrodynamic diameter (left) and PDI (right). Data represent three technical replicates (dots) as means (gray bars) ± standard error of the mean (error bars). Horizontal dashed lines represent the upper acceptable limits.

DLS analysis of nanoparticles formulated with 4 HDT and 200 ssDNA per core revealed monostability defined as mean hydrodynamic diameter of 97.2±18nm, PDI of 0.245±0.018 and zeta potential of -18.1±0.31mV (Figure 2A).

We next evaluated HDT-CRISPR-AuNP stability after centrifugation to remove excipient cargo. We previously demonstrated two rounds of centrifugation-based washing are sufficient to remove detectable, unbound cargo as visualized by sodium dodecyl sulfate polyacrylamide gel

electrophoresis (SDS-PAGE) [135]. The optimized nanoformulation maintained monostability after two rounds of spin purification, with a diameter increase to 120.5±14.72nm with PDI of 0.287±0.046 and zeta potential of -20.71±0.29mV (Figure 2A). Transmission electron microscopy (TEM) images of HDT-CRISPR-AuNP stained with uranyl acetate show distinct attachment of long dsDNA to gold cores at the HDT-AuNP stage (Figure 2B). Following complete assembly, we can also visualize polyplex corona and excess polymer in the unpurified stage, and a combination of long dsDNA and polyplex attachment to the gold core in the purified stage (Figure 2B).

For unpurified nanoparticles, Cas9 nuclease loading was determined by SDS-PAGE to be 47.12±9.93pmol, and HDT loading was determined via agarose gel electrophoresis to be 105.1±10.86ng HDT per 20ug AuNP dose (Figure 2C). Despite the increased hydrodynamic diameter observed following centrifugation, purified particles demonstrated 16.84±7.48pmol RNP with 75.58±15.46ng HDT (Figure 2C). HDT-AuNP alone carried ~400ng HDT indicating either significant displacement of the HDT from the gold surface by competing thiolated moieties, or sequestration of the HDT in the polymer matrix rendering it unavailable for charge-based gel imaging (Figure 2C).

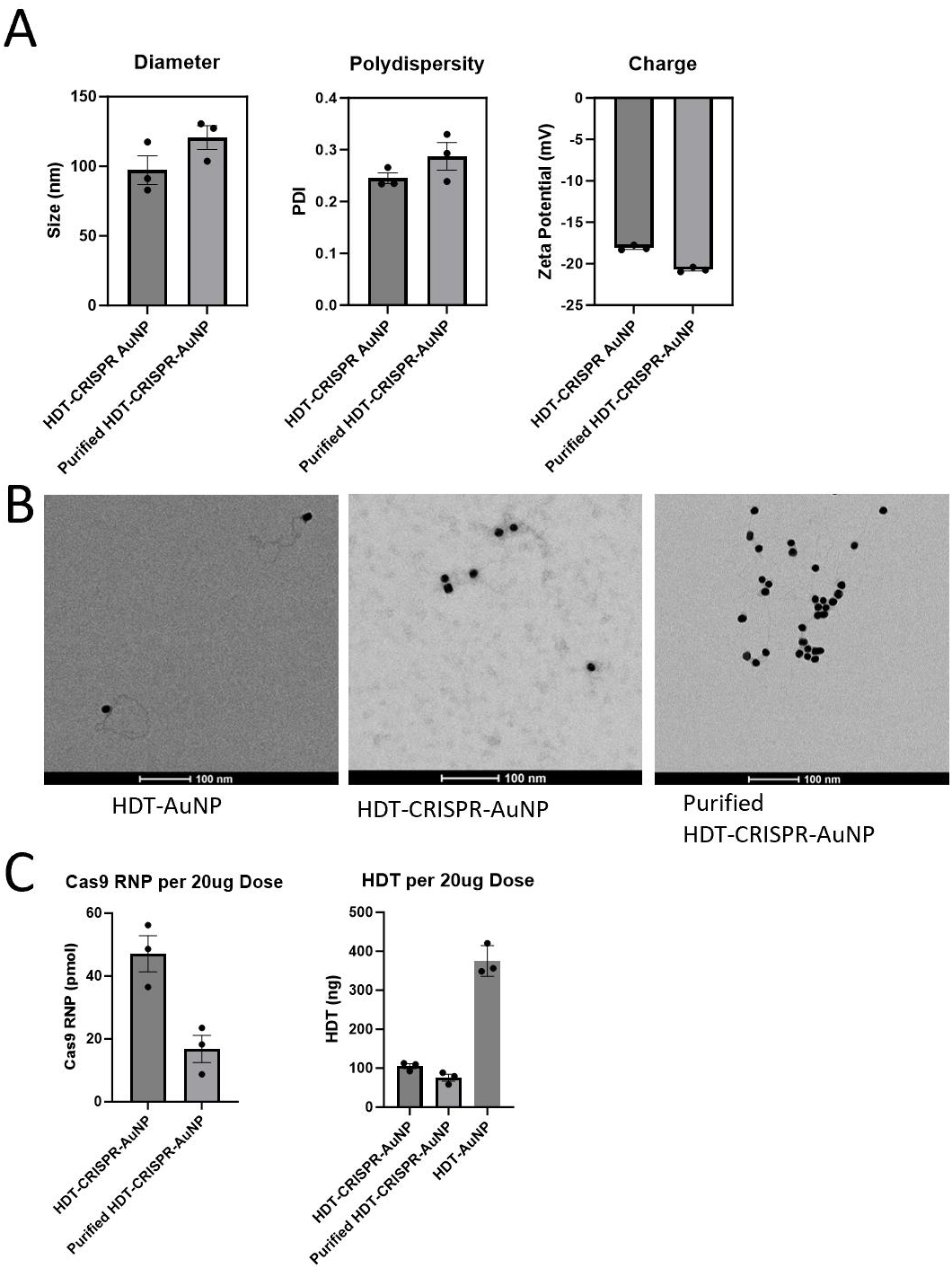

Figure 2. Purification of HDT-CRISPR-AuNP results in decreased cargo loading despite increased hydrodynamic diameter by both DLS and TEM*. (A) DLS analysis of hydrodynamic diameter (left), PDI (middle), and zeta potential (i.e. surface charge) (right). Data represent three*

technical replicates (dots) as means (gray bars) ± standard error of the mean (error bars). Horizontal dashed lines represent the upper acceptable limits. (B) Transmission electron microscopy (TEM) images of uranyl acetate stained HDT-AuNP (left), unpurified HDT-CRISPR-AuNP (middle), and purified HDT-CRISPR-AuNP (right) at 92000X magnification. (C) Graphical representation of densitometric analysis of gel images for Cas9 protein (left) and HDT (right). Data represent three technical replicates (dots) as means (gray bars) ± standard error of the mean (error bars).

In vitro validation of CRISPR-AuNP Efficacy in Jurkat Cells:

We first tested activity of unpurified HDT-CRISPR-AuNP carrying a GFP reporter transgene regulated by a minimal cytomegalovirus (CMV) promoter with homology arms to the *B2M* cut site in Jurkat cells. Jurkat cells are a human T cell line derived from acute T cell leukemia and are commonly used to evaluate CRISPR delivery prior to experiments in primary human T cells [139]. We and others have shown that CRISPR activity at the *B2M* locus results in mutations which in turn cause protein misfolding and loss of expression of B2M at the cell surface [135, 140]. The optimal B2M gRNA was selected based on protein knockdown measured by flow cytometry following electroporation of Cas9 RNP. We treated Jurkat cells with HDT-CRISPR-AuNP targeting *B2M* at a dose of 20μg AuNP and analyzed resulting loss of B2M and gain of GFP by flow cytometry. Flow analysis showed significant B2M protein knockdown in cells treated with both CRISPR-AuNP and HDT-CRISPR-AuNP (Figure 3A), as well as statistically significant GFP transgene expression from both HDT-polyplex-treated and HDT-CRISPR-AuNP-treated cells (Figure 3B). Sequencing analysis revealed insertion and deletion (indel) mutations at the target

B2M locus (Figure 3C), though not to a statistically significant extent. Importantly, nanoparticle treatment had no discernable effect on cell viability (Figure 3D).

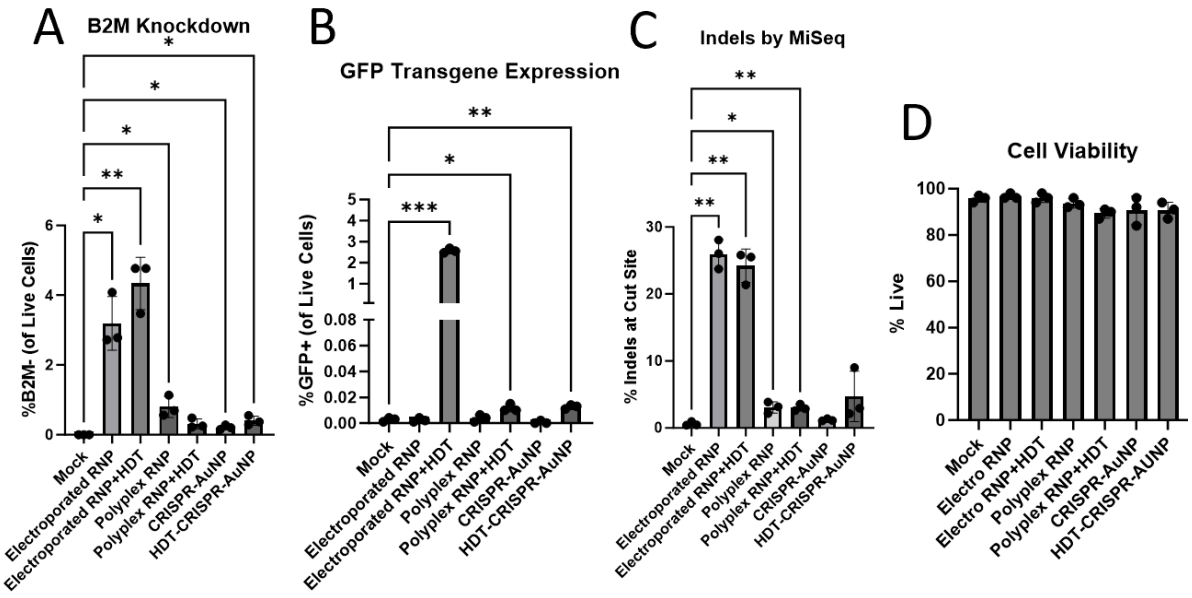

Figure 3. Treatment of Jurkat cells with HDT-CRISPR-AuNP results in gene editing and transgene expression. *(A) Flow cytometry analysis of B2M knockdown in Jurkat cells treated with HDT-CRISPR-AuNP. Cells were harvested for analysis after 4 days in culture. Data represent three technical replicates (dots) as means (gray bars) ± standard error of the mean (error bars). (B) Flow cytometry analysis of GFP transgene expression in Jurkat cells treated with HDT-CRISPR-AuNP. Data represent three technical replicates (dots) as means (gray bars) ± standard error of the mean (error bars). (C) Analysis of MiSeq reads generated from gDNA isolated from Jurkat cells. Data represent three technical replicates (dots) as means (gray bars) ± standard error of the mean (error bars) (D) Cell viability of treated Jurkats after 4 days in culture. Data represent three technical replicates (dots) as means (gray bars) ± standard error of the mean (error bars)*

CRISPR-AuNP Efficacy in Primary T Cells:

Following successful editing and transgene expression in Jurkat cells, the same *B2M*-targeted nanoparticle carrying a CMV-GFP reporter transgene was tested in primary human naïve T cells (CD3+CD45RA+CD45RO-CD197+). In brief, cells were thawed and rested overnight prior to electroporation of addition of HDT-CRISPR-AuNP or polyplex to serum-free media. After 4 days in culture, cells were harvested for analysis. Here we tested both unpurified and purified HDT-CRISPR-AuNP to determine whether editing was a result of free polyplex in solution rather than assembled HDT-CRISPR-AuNP. Flow cytometry demonstrated evident, but not statistically significant B2M knockdown and GFP expression (Figure 4A,B), while sequencing results indicated statistically significant indel levels of 6.23 ± 1.90% and 6.49 ± 3.20% in cells treated with both unpurified and purified HDT-CRISPR-AuNP, respectively (Figure 4C). Cell viability was lower across all sample sets than observed in Jurkats (compare Figure 4D with Figure 3D), with purified, but not unpurified HDT-CRISPR-AuNP showing statistically significant differences in viability between nanoparticle-treated samples and mock-treated samples (Figure 4D).

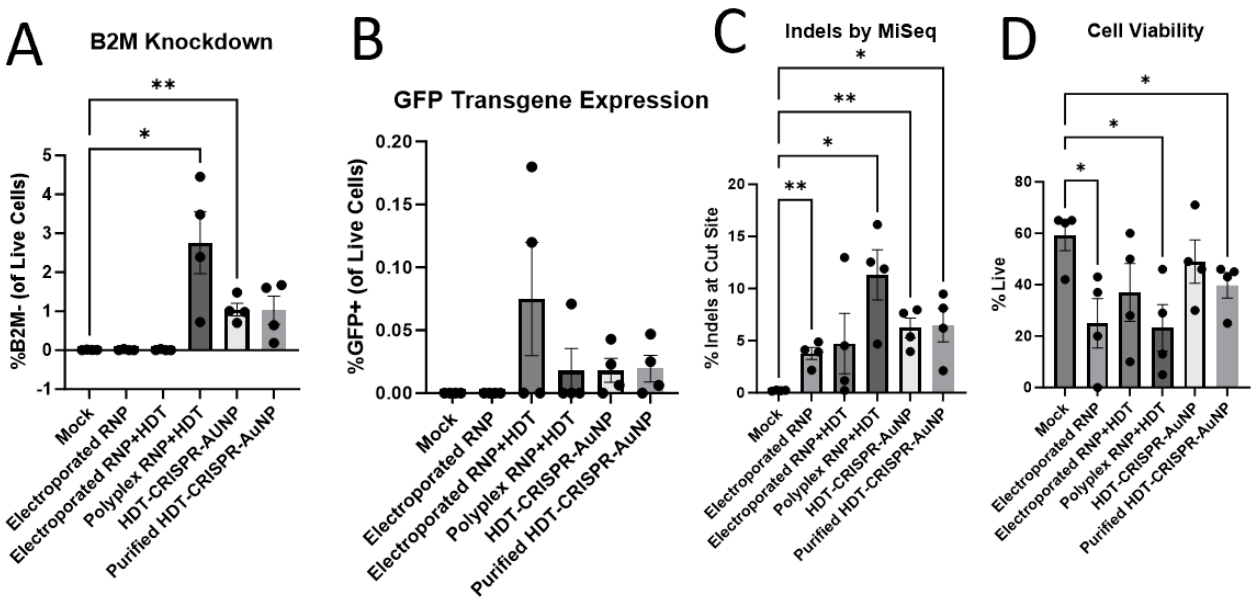

Figure 4. Treatment of primary naïve T cells with HDT-CRISPR-AuNP results in gene editing and transgene expression. *(A) Flow cytometry analysis of B2M knockdown in primary T cells treated with HDT-CRISPR-AuNP. Representative dot plots show gating of B2M- populations on live cells. Data represent four biological replicates (dots) as means (gray bars) ± standard error of the mean (error bars). (B) Flow cytometry analysis of GFP transgene expression in T cells treated with HDT-CRISPR-AuNP. Representative dot plots show gating of GFP+ populations on live cells. Data represent four biological replicates (dots) as means (gray bars) ± standard error of the mean (error bars). (C) Analysis of MiSeq reads generated from gDNA isolated from T cells. Data represent four biological replicates (dots) as means (gray bars) ± standard error of the mean (error bars) (D) Cell viability after 4 days in culture. Data represent four biological replicates (dots) as means (gray bars) ± standard error of the mean (error bars).*

Nanoparticle-mediated Immune Engineering of Primary T and CD34+ Cells:

We next sought to distinguish transgene expression in Jurkat and naïve T cells resulting from translation of exogenous double-stranded template DNA in the cytoplasm from endogenously

integrated HDT. To this end we formulated HDT-CRISPR-AuNP with a new gRNA targeting the *T cell receptor alpha constant region* (*TRAC*), and an HDT encoding an antigen-specific TCR for the New York esophageal squamous cell carcinoma 1 (NY-ESO-1) neoantigen [69, 141]. The transgene encoded in this HDT sequence consists of the full-length beta (β) chain and variable alpha (α) chain of the TCR, meaning no expression of the transgenic TCR will occur unless it is inserted correctly downstream of the endogenous *TCR-α* promoter [69]. HDT-CRISPR-AuNP synthesized with these novel elements were stable and monodisperse (Figure 5A).

Having established that HDT-CRISPR-AuNP can be synthesized with modular HDT and gRNA cargo, we sought to determine where the nanoparticles trafficked in primary cells. Tracing cell uptake and endosomal escape lends us a better understanding of the mechanisms by which nanoparticles are endocytosed by the cells and therefore lets us know whether we are achieving endosomal escape or if any observed editing is the result of low-level leakage of gene editing cargo from intact endosomes. We utilized fluorescently tagged cargo to track HDT-CRISPR-AuNP uptake in T cells using confocal microscopy. We synthesized HDT-CRISPR-AuNP with a fluorescent ATTO550 tag conjugated to the tracrRNA portion of the gRNA, which colocalizes with RNP. Fluorescently-labeled HDT-CRISPR-AuNP maintained stability as measured by DLS (Figure 5B). Confocal microscopy demonstrated diffuse ATTO550 fluorescence throughout the cell cytoplasm and nucleus, indicating that at least tracrRNA cargo are capable of cellular entry, endosomal escape and nuclear entry (Figure 6), though treatment with purified nanoparticles results in lower fluorescence in the cells imaged, in line with results from protein-loading characterization assays (Figure 2C).

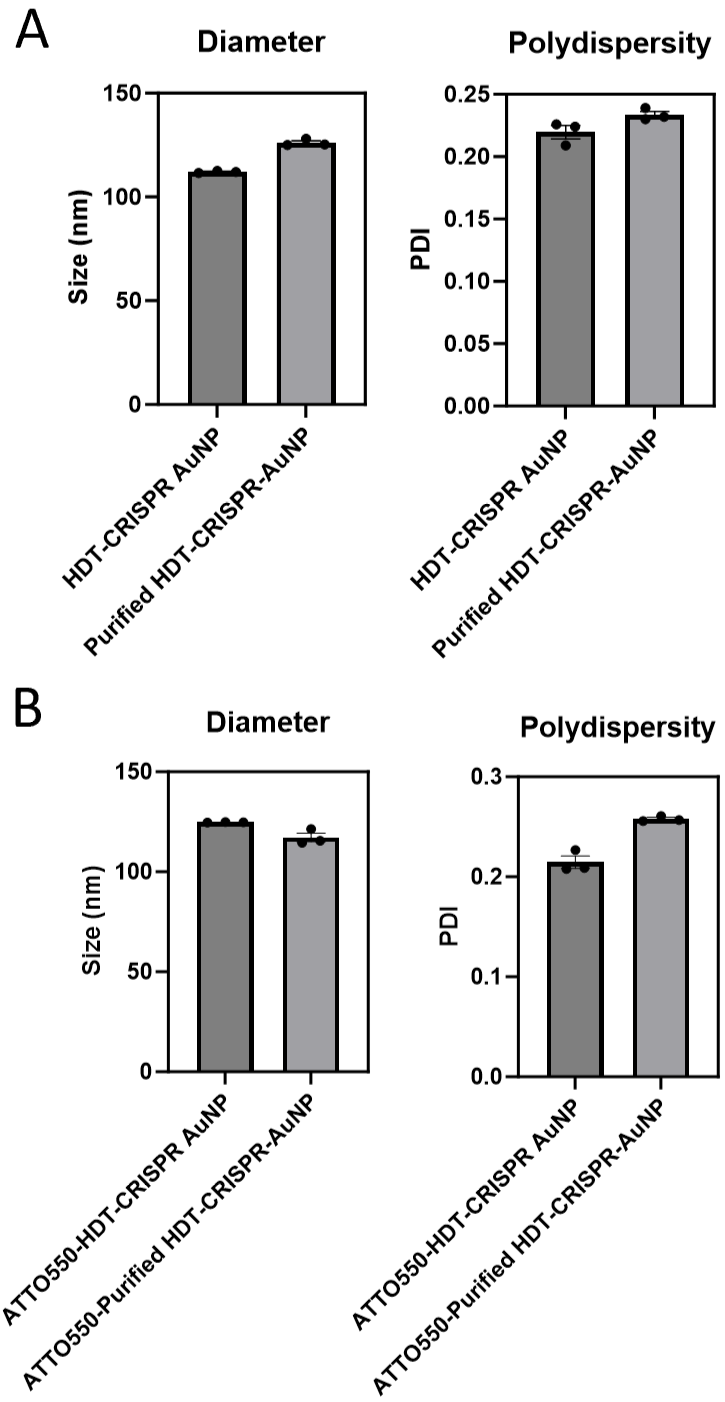

Figure 5. HDT-CRISPR-AuNP formulated with alternate gRNA and HDT maintain monostability.

(A) *HDT-CRISPR-AuNP formulated with TRAC-targeted gRNA and a 2.1kb HDT containing an antigen-specific TCR demonstrate acceptable size and monostability in both purified and non-*

purified formulations. Data represent three technical replicates (dots) as means (gray bars) ± standard error of the mean (error bars). (B) The TRAC HDT-CRISPR-AuNP formulated with a fluorescently labeled ATTO550 tracrRNA are monostable. Data represent three technical replicates (dots) as means (gray bars) ± standard error of the mean (error bars).

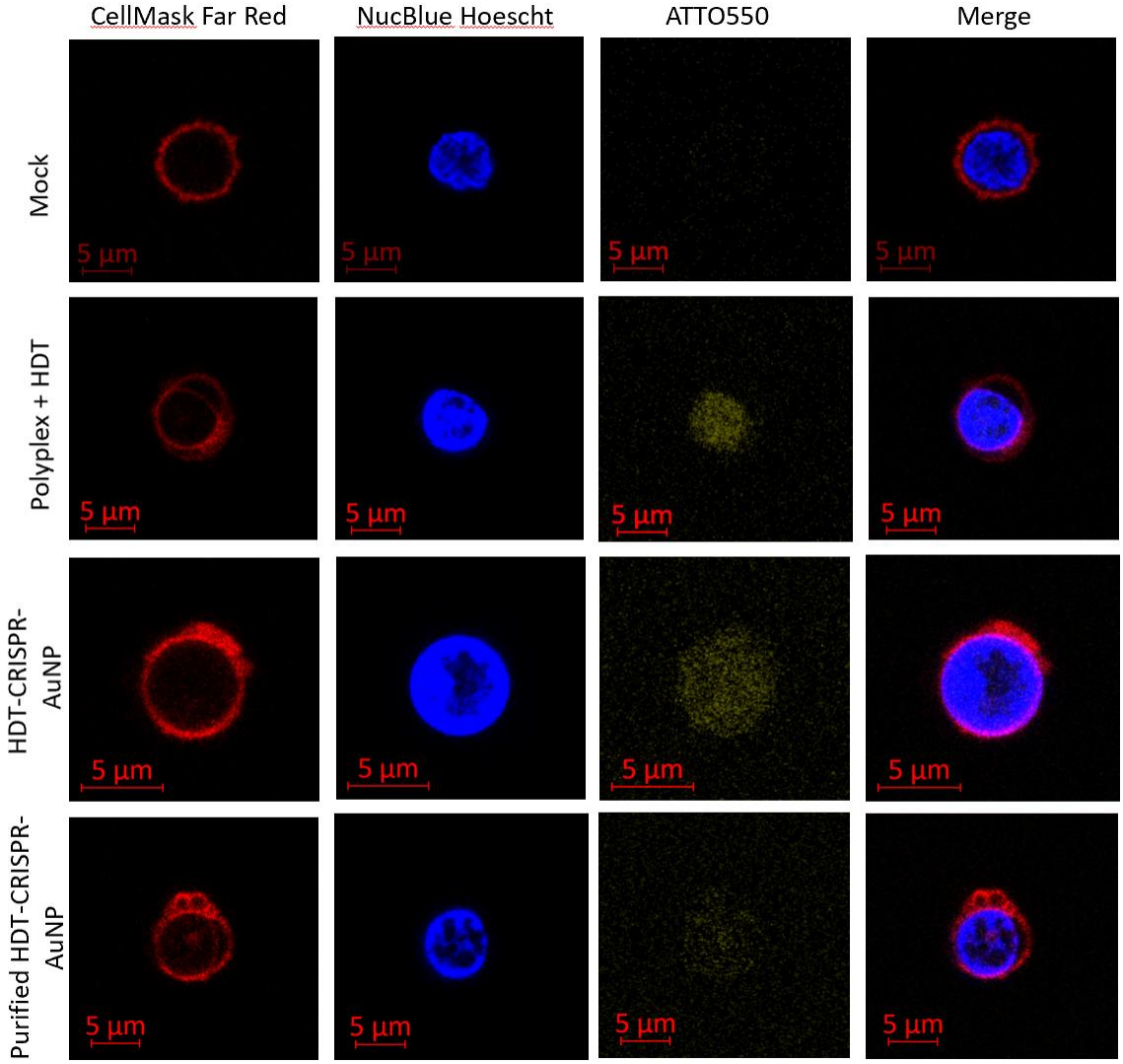

Figure 6. Confocal microscopy on T Cells treated with fluorescently labeled HDT-CRISPR-AuNP shows endosomal escape and nuclear entry. *Primary T cells treated with HDT-CRISPR-AuNP formulated using a tracrRNA tagged with ATTO550 (yellow) and labeled with CellMask Far Red*

Membrane Dye (red) and NucBlue Nuclear Stain (blue) were imaged at 64X by confocal microscope. Images representative of 3 biological replicates.

Non-fluorescently labeled HDT-CRISPR-AuNP were used to treat primary human T cells in culture. Following treatment with 20ug unpurified or purified HDT-CRISPR-AuNP, pan CD3+ T cells did not show statistically significant knockout of endogenous TCR alpha-beta chain, but did demonstrate some editing at the target site by next-generation sequencing (Figure 7A,C). However dextramer binding to NY-ESO-1 TCR on the cell surface was not observed above background for any treated sample (Figure 7B). Notably, low dextramer binding was also observed in electroporated positive controls. Further testing in an NY-ESO-1 expressing cell line demonstrated faulty dextramer (Figure 8).

In the absence of confirmation of HDR by protein expression, we instead designed a PCR assay wherein the forward primer bound in the *TRAC* locus upstream of the 5' homology arm of the HDT and the reverse primer bound within the variable beta chain sequence of the TCR transgene. PCR on a genomic DNA (gDNA) sample that contains the integrated insert should therefore yield 645bp product, while gDNA with no integrated HDT should yield no product (Figure 7E). Additionally, this assay cannot amplify exogenous HDT. PCR products from cells electroporated with RNP and HDT, as well as cells treated with unpurified HDT-CRISPR-AuNP, showed faint bands of the expected length (Figure 7F). Sanger sequencing of bands demonstrated upwards of 95% homology to the target 645bp band (data not shown), indicating

successful, low level, integration of the transgene into the target locus. No other sample set, including RNP+HDT polyplex-treated cells and purified HDT-CRISPR-AuNP-treated cells, demonstrated visible PCR products in this assay.

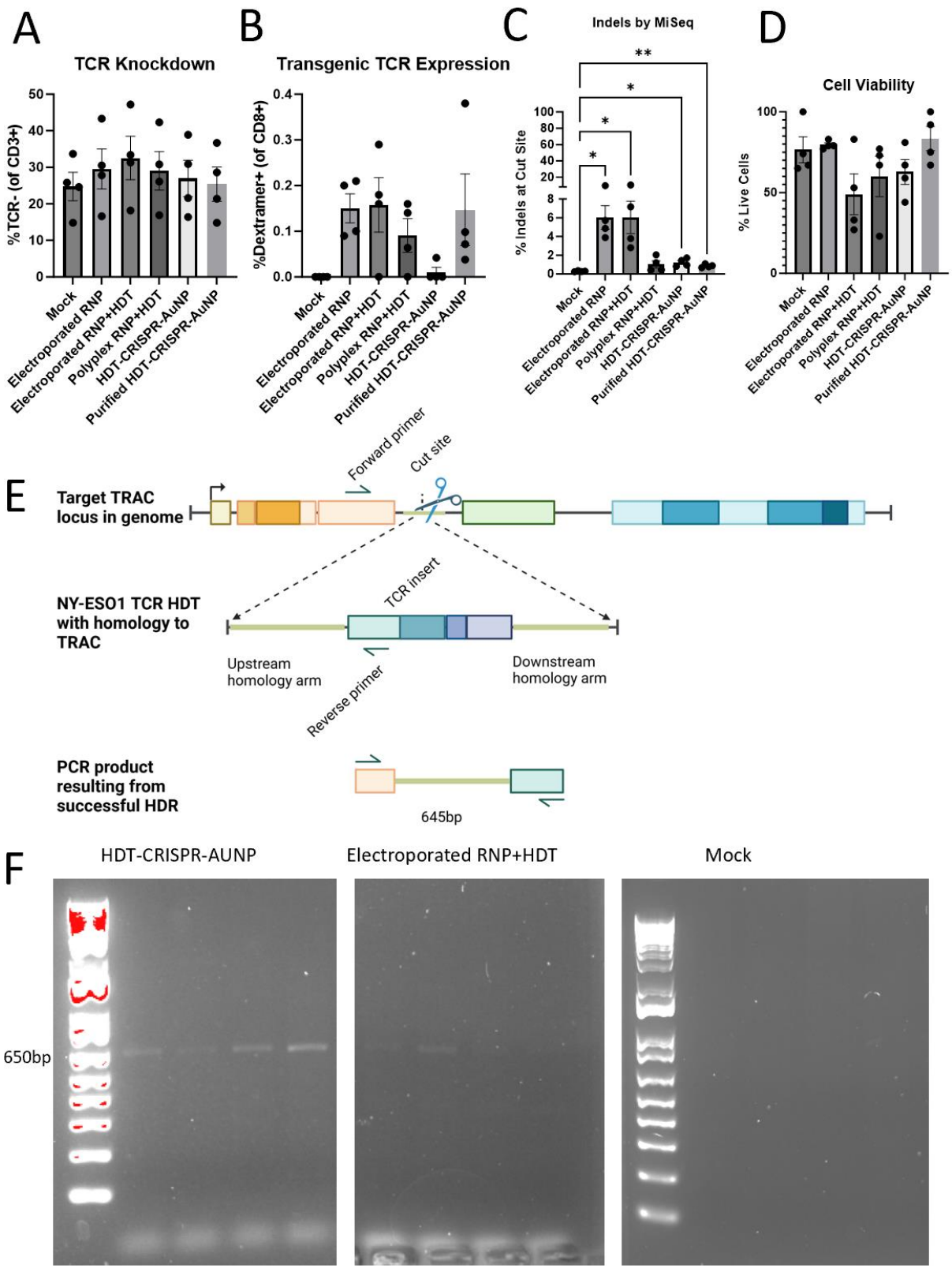

Figure 7. Primary T cells treated with TRAC-targeted HDT-CRISPR-AuNP carrying a transgenic

TCR HDT showed gene editing and suggested successful HDR, but no transgene expression was detected by flow cytometry. *(A) Flow cytometry analysis of TCR knockdown in primary T cells treated with HDT-CRISPR-AuNP. Representative dot plots show gating of TCR- populations on CD3+ live cells. Data represent four biological replicates (dots) as means (gray bars) ± standard error of the mean (error bars). (B) Flow cytometry analysis of transgenic TCR expression in T cells treated with HDT-CRISPR-AuNP. Representative dot plots show gating of GFP+ populations on live cells. Data represent four biological replicates (dots) as means (gray bars) ± standard error of the mean (error bars). (C) Analysis of MiSeq reads generated from gDNA isolated from T cells. Data represent four biological replicates (dots) as means (gray bars) ± standard error of the mean (error bars) (D) Cell viability after 4 days in culture. Data represent four biological replicates (dots) as means (gray bars) ± standard error of the mean (error bars) (E) Schematic of integration PCR performed on gDNA from treated T cells. (F) Agarose gel images showing integration PCR product presence in positive control and HDT-CRISPR-AuNP samples and absence in mock sample gDNA.*

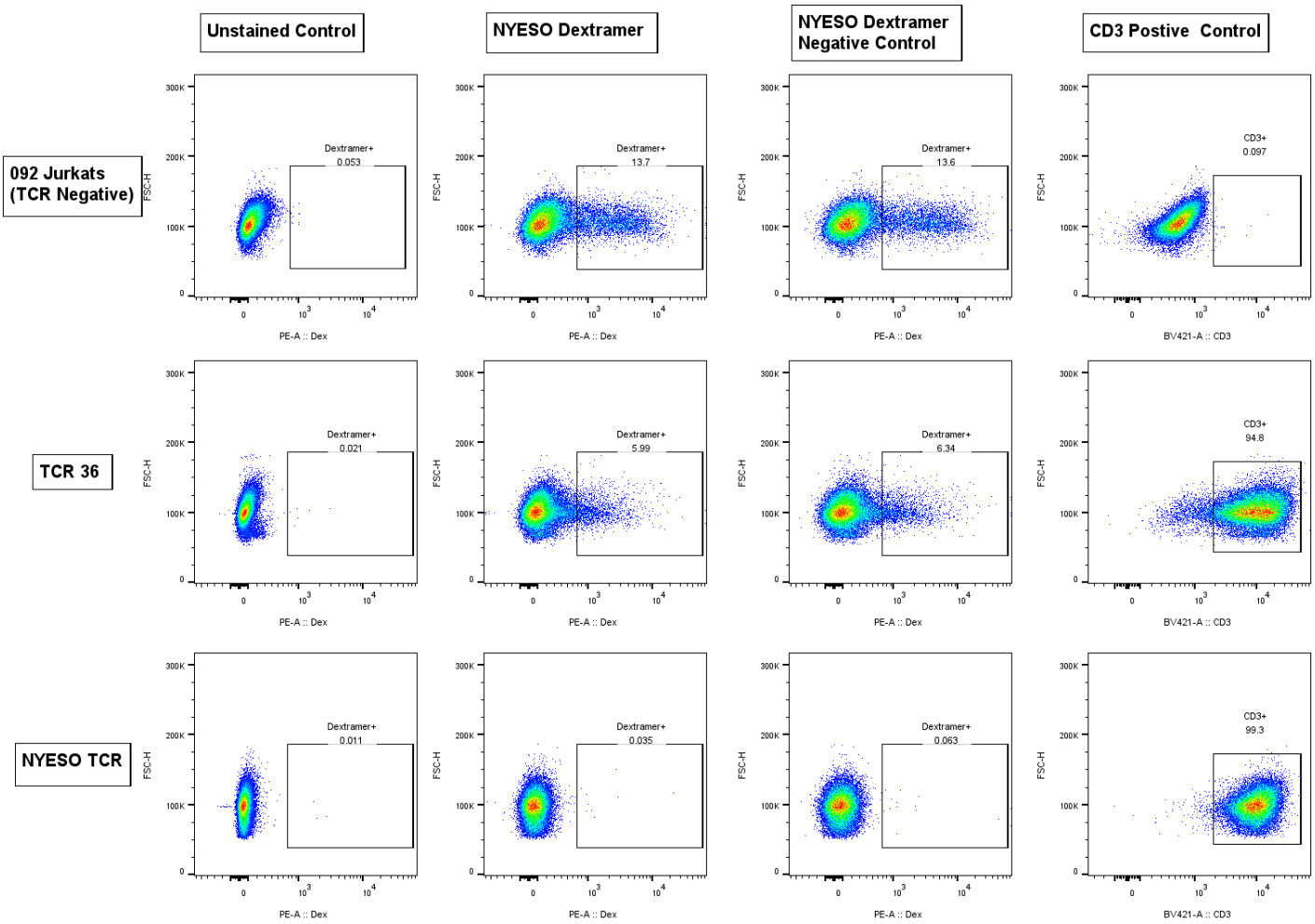

Figure 8. Dextramer staining of NY-ESO-1-specific TCR engineered Jurkat line shows faulty binding. *Flow cytometry analysis of Jurkat cells engineered to express no (top row), non-specific (middle row) or NY-ESO-1-specific TCR (bottom row).*

TRAC-targeted HDT-CRISPR-AuNP carrying the *NY-ESO-1 TCR* construct were also used to treat primary human CD34+ HSPC in vitro. HSPC do not express TCR, but at least one study showed that HSPC edited with CAR transgenes express these transgenes after differentiation into a T cell lineage [92] . The endogenous TCRα promoter is inactive in HSPC, meaning no transgene

expression would be expected on the surface of CD34+ cells even if HDR occurred. As such, gDNA was extracted from each sample and subjected to gDNA sequencing as well as the integration PCR assay we developed described above. Sequencing showed up to 5.08% indels at the *TRAC* locus for HDT-CRISPR-AuNP but fell short of statistical significance (Figure 9A). Cell viability remained high regardless of treatment, with no statistical difference between mock-treated cells and any treated sample (Figure 9B). Integration PCR showed bands at the expected length for all four of the electroporated RNP+HDT samples, and for two of the HDT-CRISPR-AuNP samples (Figure 9C), with no bands for any of the other sample sets. Altogether this data indicate that HDT-CRISPR-AuNP are active in both primary human T cells and HSPC.

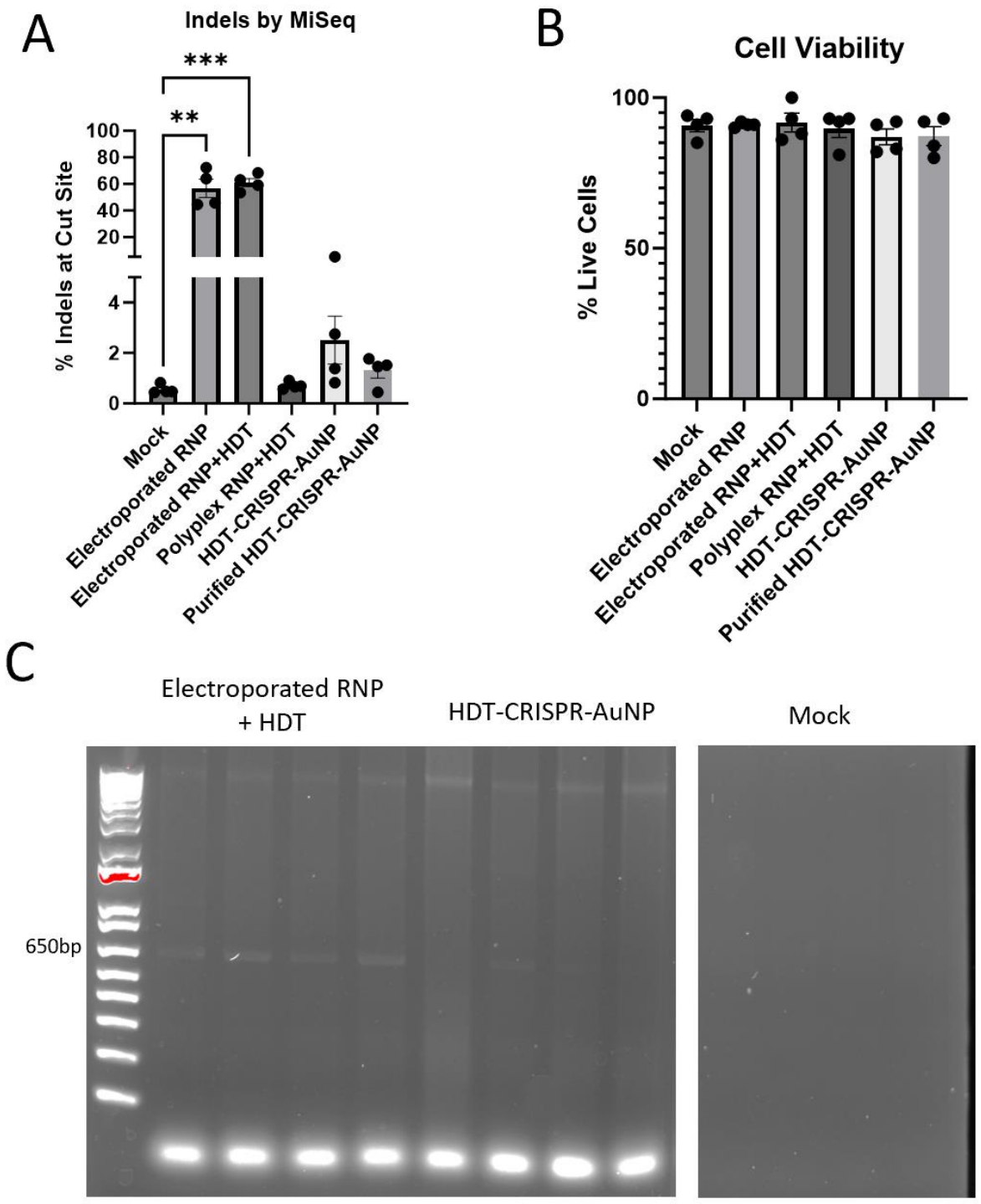

Figure 9. CD34+ HSPC treated with TRAC-targeted HDT-CRISPR-AuNP carrying a transgenic TCR HDT showed gene editing and integration of HDT. (A) *Analysis of MiSeq reads generated from gDNA isolated from CD34+ cells. Data represent four biological replicates (dots) as means*

(gray bars) ± standard error of the mean (error bars) (D) Cell viability after 4 days in culture. Data represent four biological replicates (dots) as means (gray bars) ± standard error of the mean (error bars)(C*) Agarose gel images showing integration PCR product presence in positive control and HDT-CRISPR-AuNP samples and absence in mock sample gDNA.*

Discussion:

Developing an inexpensive technology that can deliver therapeutic transgenes into blood cells is a goal that if reached has widespread implications for primary hematopoietic cell engineering at large. In addition to producing TCR-T and CAR-T cell products or creating a self-renewing reservoir of HSPC that mature into transgenic T cells, such technology could be used to generate B cells that produce transgenic antibody, or plasma cells that generate any number of secreted therapeutic proteins [92, 142, 143]. A non-viral, synthetic delivery platform which does not require complicated protein engineering that can co-deliver Cas9 RNP and long transgenes promises to lower the barriers of cost and accessibility. In contrast to other gold nanoparticle-based CRISPR delivery platforms, HDT-CRISPR-AuNP maintains stability post-purification [144] and shows limited toxicity [131, 144]. HDT-CRISPR-AuNP does not require filtration after synthesis, maintains stability with simple centrifugation, and is capable of loading HDT >2000bp, in contrast to other gold nanoparticle and LNP platforms [128, 144]. Synthesis is a cell-free process, in contrast to eVLP and viral systems [120]. Importantly, HSPC treated with HDT-CRISPR-AuNP maintain excellent viability and require less than 100pmol CRISPR RNP to mediate gene editing, indicating an advantage over peptide-based delivery systems [145].

We have shown here that HDT-CRISPR-AuNP is capable of RNP and DNA co-delivery to target cells in vitro, but the possibility of in vivo efficacy is a serious consideration. Currently, there are few FDA-approved gold nanomedicines, including PEG-functionalized gold nanorods used for tumor ablation (Auralase™) [146]. Gold nanoparticles have been used in the past to treat inflammatory diseases like arthritis [147]. Short interfering RNA (siRNA) coated AuNP have been shown to be well-tolerated in a clinical trial for glioblastoma [148]. The potential of AuNP for in vivo efficacy as a gene editing platform has been shown by other research groups. Lee et al. demonstrated in vivo efficacy of RNP-functionalized gold nanoparticles in a murine model of muscular dystrophy via HDR using a <200bp DNA template [128]. The base CRISPR-AuNP formulation consisting of the gold core, CRISPR RNP and thiolated PEI-PEG polymer without conjugated transgenes has shown little to no toxicity in vitro. In vivo testing will demonstrate whether HDT-CRISPR-AuNP may be capable of safely delivering DNA transgenes in addition to CRISPR gene editing in the context of more complex physiology.

dsDNA has shown some cytotoxicity when delivered to the cell cytoplasm via electroporation [69]. It is likely that HDT-CRISPR-AuNP mediates less toxicity than electroporation in most treated cell types due to the low concentration of dsDNA delivered, which in turn results in lower transgene expression than electroporated samples. While transgene expression from cells edited with HDT-CRISPR-AuNP is relatively low, in many contexts the transduction of only a few cells is sufficient to mediate an appropriate immune response [149]. Further optimization of nanoparticle cargo, including alternate CRISPR nucleases, may increase transgene integration efficiency. As with the base particle, it is likely that HDT-CRISPR-AuNP can be modified to carry an array of different CRISPR nucleases for different purposes. So long as one of the nucleic acids

involved is amenable to modification with a thiol-spacer group, engineered nucleases such as prime editors [54], as well as eePASSIGE and CAST recombinase-based gene editing systems [55, 56] should be compatible with CRISPR-AuNP synthesis. These would benefit from being delivered as RNP due to the multiple proteins and lengthy RNAs that comprise these systems [54-56]. Conjugating highly optimized, engineered gene editing technologies to HDT-CRISPR-AuNP is likely to increase the efficacy of the platform for integrating large genes into target loci. Continued research into gold-core nanoparticles and their ability to simultaneously deliver multiple cargo types into cells may yield valuable new treatments for diseases of the genome while increasing the accessibility of gene therapy for all. The development of our simple particle design which can be manufactured in a standard laboratory setting at low cost in a short time and with commercially available materials should accelerate research and clinical development more broadly.

Conclusion:

In this proof of concept study, we demonstrate across several cell types and with two different transgenes the ability to deliver CRISPR-based gene editing and transgene insertion at two different loci by non-viral HDT-CRISPR-AuNP. While the efficiency of gene editing induced by HDT-CRISPR-AuNP is quite low compared to viral transduction or electroporation, existing data on the CRISPR-AuNP base platform suggests a high potential for in vivo use, and at a fraction of the cost of viral therapies. Future studies in humanized mouse models may support the use of HDT-CRISPR-AuNP for in vivo stem cell and immune cell engineering.

Methods:

Materials:

All PCR primers and gRNAs were purchased from IDT (Coralville, Iowa, US). CMV-GFP reporter plasmids were synthesized by and purchased from GenScript USA (Piscataway, New Jersey, US). NY-ESO-1 TCR plasmid was a gift from Alexander Marson (Addgene plasmid # 207482 ; http://n2t.net/addgene:207482 ; RRID:Addgene_20748). SpCas9 nuclease was purchased from Aldevron (Fargo, North Dakota, US). Chloroauric acid, sodium citrate dibasic trihydrate, hydrochloric acid, and β-mercaptoethanol (BME) were purchased from Sigma-Aldrich (St. Louis, Missouri, US). Neon™ Electroporation System 100µL Kit (Invitrogen, Waltham, MA, USA) was used on the Neon Transfection System (Invitrogen) for all electroporations. Flow cytometry antibodies were purchased from Biolegend (San Diego, California, US). MHC dextramer was purchased from Immudex (Copenhagen, Denmark). PEI-PEG copolymers were purchased from Nanosoft Polymers (Winston-Salem, NC, US). Other materials not listed were purchased through ThermoFisher Scientific (Waltham, Massachusetts, US).

Nanoparticle Synthesis:

Nanoparticle synthesis involves less than 2 hours of hands-on time. AuNP of 15-20nm in diameter are first synthesized using the Turkevich method [134] and then characterized via TEM (TALOS120C, ThermoFisher Scientific) and visible ultraviolet (UV-Vis) absorbance at 520nm wavelength (Nanodrop One, ThermoFisher Scientific) [135] to accurately estimate nanoparticle molarity for binding cargo. AuNP molarity was calculated using 1 cm Beer–Lambert law absorbance at 520 nm as previously described by Lane et, al [135]. AuNP are then incubated

with thiol-oligoethylene glycol-modified HDT encoding a transgene construct with 300bp homology arms (Table 1). HDT is added at a 4:1 molar ratio and a similarly modified 25nt ssDNA at a 200:1 molar ratio in the presence of 25mM citrate buffer. The short ssDNA coats the remainder of the gold surface and prevents aggregation of gold particles in the presence of citrate buffer. For the sake of replicability, different batches of AuNP were diluted to have equivalent molarities such that the amount of HDT loaded into a 20ug dose of AuNP was consistently 4ug dsDNA. After incubation with thiol-modified DNA, HDT-AuNP are washed twice by centrifugation at 15,000RCF at 4C for 45 minutes at to remove unbound DNA. Meanwhile, 100pmol Cas9 RNP is formed by combining Cas9 protein and thiol-modified gRNA at a 1:1 ratio. This thiolated RNP is combined with 10ug 2000W-graft-20 PEI-PEG thiolated polymer to form an RNP polyplex, by incubating at room temperature for one hour prior to HDT-AuNP addition and vigorous trituration for 10 seconds. Final formulations were stored at 4C for up to 3 days.

Name	Oligonucleotide sequence
HDT Sequences	
B2M CMV-GFP HDT	GGGAAAGATACCAAGTCACGGTTTATTCTTCAAAATGGAGGTGGCTTGTTGGGAAGG TGGAAGCTCATTTGGCCAGAGTGGAAATGGAATTGGGAGAAATCGATGACCAAATGT AAACACTTGGTGCCTGATATAGCTTGACACCAAGTTAGCCCCAAGTGAAATACCCTGGC AATATTAATGTGTCTTTTCCCGATATTCCTCAGGTACTCCAAAGATTCAGGTTTACTCACG TCATCCAGCAGAGAATGGAAAGTCAAATTTCCTGAATTGCTATGTGTCTGGGTTTCATC CATCCGACACGTTACATAACTTACGGTAAATGGCCCGCCTGGCTGACCGCCCAACGACC CCCGCCCATTGACGTCAATAATGACGTATGTTCCCATAGTAACGCCAATAGGGACTTTCC ATTGACGTCAATGGGTGGAGTATTTACGGTAAACTGCCCACTTGGCAGTACATCAAGT GTATCATATGCCAAGTACGCCCCCTATTGACGTCAATGACGGTAAATGGCCCGCCTGGC ATTATGCCCAGTACATGACCTTATGGGACTTTCCTACTTGGCAGTACATCTACGTATTAGT CATCGCTATTACCATGGTGATGCGGTTTTGGCAGTACATCAATGGGCGTGGATAGCGGT TTGACTCACGGGGATTTCCAAGTCTCCACCCCATTGACGTCAATGGGAGTTTGTTTTG GCACCAAAATCAACGGGACTTTCCAAAATGTCGTAACAACTCCGCCCCATTGACGCAA ATGGGCGGTAGGCGTGTACGGTGGGAGGTCTATATAAGCAGAGCTGGTTTAGTGAAC CGTCAGATCCGCTAGCGCTACCGGTCGCCACCATGGTGAGCAAGGGCGAGGAGCTGT TCACCGGGGTGGTGCCCATCCTGGTCGAGCTGGACGGCGACGTAAACGGCCACAAGT

	TCAGCGTGTCCGGCGAGGGCGAGGGCGATGCCACCTACGGCAAGCTGACCCTGAAG TTCATCTGCACCACCGGCAAGCTGCCCGTGCCCTGGCCCACCCTCGTGACCACCCTGA CCTACGGCGTGCAGTGCTTCAGCCGCTACCCCGACCACATGAAGCAGCACGACTTCTT CAAGTCCGCCATGCCCGAAGGCTACGTCCAGGAGCGCACCATCTTCTTCAAGGACGAC GGCAACTACAAGACCCGCGCCGAGGTGAAGTTCGAGGGCGACACCCTGGTGAACCG CATCGAGCTGAAGGGCATCGACTTCAAGGAGGACGGCAACATCCTGGGGCACAAGCT GGAGTACAACTACAACAGCCACAACGTCTATATCATGGCCGACAAGCAGAAGAACGG CATCAAGGTGAACTTCAAGATCCGCCACAACATCGAGGACGGCAGCGTGCAGCTCGC CGACCACTACCAGCAGAACACCCCCATCGGCGACGGCCCCGTGCTGCTGCCCGACAA CCACTACCTGAGCACCCAGTCCGCCCTGAGCAAAGACCCCAACGAGAAGCGCGATCA CATGGTCCTGCTGGAGTTCGTGACCGCCGCCGGGATCACTCTCGGCATGGACGAGCTG TACAAGTAGAGCGGCCGCGGGGATCCAGACATGATAAGATACATTGATGAGTTTGGAC AAACCACAACTAGAATGCAGTGAAAAAAATGCTTTATTTGTGAAATTTGTGATGCTATT GCTTTATTTGTAACCATTATAAGCTGCAATAAACAAGTTAACAACAACAATTGCATTCAT TTTATGTTTCAGGTTCAGGGGGAGGTGTGGGAGGTTTTTTTAAGATTGAAGTTGACTT ACTGAAGAATGGAGAGAGAATTGAAAAAGTGGAGCATTCAGACTTGTCTTTCAGCAA GGACTGGTCTTTCTATCTCTTGTACTACACTGAATTCACCCCCACTGAAAAAGATGAGT ATGCCTGCCGTGTGAACCATGTGACTTTGTCACAGCCCAAGATAGTTAAGTGGGGTAA GTCTTACATTCTTTTGTAAGCTGCTGAAAGTTGTGTATGAGTAGTCATATCATAAAGCTG CTTTGATATAAAAAAGGTCTATGGCCATACTACCCTGAATGAGTCCCATCC
TRAC NY-ESO-1 TCR HDT	TTTCAGGTTTCCTTGAGTGGCAGGCCAGGCCTGGCCGTGAACGTTCACTGAAATCATG GCCTCTTGGCCAAGATTGATAGCTTGTGCCTGTCCCTGAGTCCCAGTCCATCACGAGCA GCTGGTTTCTAAGATGCTATTTCCCGTATAAAGCATGAGACCGTGACTTGCCAGCCCCA CAGAGCCCCGCCCTTGTCCATCACTGGCATCTGGACTCCAGCCTGGGTTGGGGCAAA GAGGGAAATGAGATCATGTCCTAACCCTGATCCTCTTGTCCCACAGATATCCAGAACCC TGACCCTGCCTCCGGATCCGGAGAGGGCAGGGGATCTCTCCTTACTTGTGGCGACGT GGAGGAGAACCCCGGCCCCATGAGCATCGGCCTCCTGTGCTGTGCAGCCTTGTCTCTC CTGTGGGCAGGTCCAGTGAATGCTGGTGTCACTCAGACCCCAAAATTCCAGGTCCTGA AGACAGGACAGAGCATGACACTGCAGTGTGCCCAGGATATGAACCATGAATACATGTC CTGGTATCGACAAGACCCAGGCATGGGGCTGAGGCTGATTCATTACTCAGTTGGTGCT GGTATCACTGACCAAGGAGAAGTCCCCAATGGCTACAATGTCTCCAGATCAACCACAG AGGATTTCCCGCTCAGGCTGCTGTCGGCTGCTCCCTCCCAGACATCTGTGTACTTCTGT GCCAGCAGTTACGTCGGGAACACCGGGGAGCTGTTTTTTGGAGAAGGCTCTAGGCTG ACCGTACTGGAGGACCTGAAAAACGTGTTCCCACCCGAGGTCGCTGTGTTTGAGCCAT CAGAAGCAGAGATCTCCCACACCCAAAAGGCCACACTGGTATGCCTGGCCACAGGCT TCTACCCCGACCACGTGGAGCTGAGCTGGTGGGTGAATGGGAAGGAGGTGCACAGT GGGGTCAGCACAGACCCGCAGCCCCTCAAGGAGCAGCCCGCCCTCAATGACTCCAGA TACTGCCTGAGCAGCCGCCTGAGGGTCTCGGCCACCTTCTGGCAGAACCCCCGCAAC CACTTCCGCTGTCAAGTCCAGTTCTACGGGCTCTCGGAGAATGACGAGTGGACCCAG GATAGGGCCAAACCCGTCACCCAGATCGTCAGCGCCGAGGCCTGGGGTAGAGCAGAC TGTGGCTTCACCTCCGAGTCTTACCAGCAAGGGGTCCTGTCTGCCACCATCCTCTATGA GATCTTGCTAGGGAAGGCCACCTTGTATGCCGTGCTGGTCAGTGCCCTCGTGCTGATG GCTATGGTCAAGAGAAAGGATTCCAGAGGCCGGGCCAAGCGGTCCGGATCCGGAGC CACCAACTTCAGCCTGCTGAAGCAGGCCGGCGACGTGGAGGAGAACCCCGGCCCCAT

	GGAGACCCTCTTGGGCCTGCTTATCCTTTGGCTGCAGCTGCAATGGGTGAGCAGCAAA CAGGAGGTGACGCAGATTCCTGCAGCTCTGAGTGTCCCAGAAGGAGAAAACTTGGTT CTCAACTGCAGTTTCACTGATAGCGCTATTTACAACCTCCAGTGGTTTAGGCAGGACCC TGGGAAAGGTCTCACATCTCTGTTGCTTATTCAGTCAAGTCAGAGAGAGCAAACAAGT GGAAGACTTAATGCCTCGCTGGATAAATCATCAGGACGTAGTACTTTATACATTGCAGC TTCTCAGCCTGGTGACTCAGCCACCTACCTCTGTGCTGTGAGGCCCCTGTACGGAGGA AGCTACATACCTACATTTGGAAGAGGAACCAGCCTTATTGTTCATCCGTATATCCAGAAC CCTGACCCTGCGGTGTACCAGCTGAGAGACTCTAAATCCAGTGACAAGTCTGTCTGCC TATTCACCGATTTTGATTCTCAAACAAATGTGTCACAAAGTAAGGATTCTGATGTGTATA TCACAGACAAAACTGTGCTAGACATGAGGTCTATGGACTTCAAGAGCAACAGTGCTGT GGCCTGGAGCAACAAATCTGACTTTGCATGTGCAAACGCCTTCAACAACAGCATTATT CCAGAAGACACCTTCTTCCCCAGCCCAGGTAAGGGCAGCTTTGGTGCCTTCGCAGGC TGTTTCCTTGCTTCAGGAATGGCCA
PCR Primers	
B2M HDT Forward Primer (FP)*	/5ThioMC6-D/iSp18/GGGAAAGATACCAAGTCACGGTTTA
B2M HDT Reverse Primer (RP)	GGATGGGACTCATTCAGGGTAGTAT
B2M MiSeq FP	GACACCAAGTTAGCCCCAA
B2M MiSeq RP	CATTCAGGGTAGTATGGCCATAG
TRAC HDT FP	/5ThioMC6-D/iSp18/TTTCAGGTTTCCTTGAGTGGC
TRAC HDT RP	TGGCCATTCCTGAAGCAAGGAAACAG
TRAC MiSeq FP	CCATCACGAGCAGCTGGTTTCTAAGATGCTA
TRAC MiSeq RP	CTGTTGCTCTTGAAGTCCATAGACCTCATGT
TRAC Integration PCR FP	TTCTGCTAATGCCCAGCCTAAG
TRAC Integration PCR RP	TGTCTTCAGGACCTGGAATTTTG
gRNA Sequences	

Cas9 B2M gRNA	/5ThioMC6-D/iSp18/rCrArGrUrArArGrUrCrArArCrUrUrCrArArUrGrUrGrUrUrUrUrArGrArGrCrUrArUrGrCrU
Cas9 TRAC gRNA	/5ThioMC6-D/iSp18/rArGrArGrUrCrUrCrUrCrArGrCrUrGrGrUrArCrAGrUrUrUrUrArGrArGrCrUrArUrGrCrU

Table 1. All oligonucleotide sequences used in nanoparticle synthesis, gene editing analysis, and PCR.

Dynamic Light Scattering Characterization

Nanoparticle solutions were suspended in ultrapure water (UPW; Invitrogen) and analyzed in using a Zetasizer Nano ZS (Malvern Panalytical, Worcestershire, UK). At least 5ug gold solution was diluted into at least 100uL UPW and loaded into 40uL disposable cuvettes (BrandTech Scientific, Connecticut, US) for size and PDI measurement. Cuvettes were allowed to equilibrate for 1 minute prior to reading with three averaged runs of 10 sub runs each. For zeta potential measurement, nanoparticle solutions were diluted in 800uL UPW and loaded into folded-capillary cuvettes (Malvern Panalytical). Charge measurements were made using autosense. Measurements for each sample were taken in triplicate at 20C.

Imaging by TEM

Fully formulated HDT-CRISPR-AuNP and HDT-AuNP were stained with 1% uranyl acetate as a negative stain to show protein, polymer, and DNA in high contrast. Grid-mounted nanoparticles were imaged using TALOS120C (ThermoFisher Scientific). For diameter calculations, TEM images were analyzed in ImageJ (Version: 1.54f) by measuring diameter on two axes for at least 20 AuNP.

RNP Loading Characterization by SDS-PAGE

2.5ug CRISPR-AuNP solution based on gold core mass was combined with 4X lithium dodecyl sulfate (LDS) loading buffer (Invitrogen, Waltham, MA, US), according to the manufacturer's instructions and incubated for 15 minutes at 95ºC. Each sample was loaded into a NuPAGE™ 4-12% Bis-Tris Mini Protein Gels (Invitrogen) and electrophoresed at 200mV for 30 minutes. Gels were stained using SimplyBlue SafeStain (Invitrogen) imaged using iBright FL1500 Imaging System (Invitrogen) and analysed for density using the iBright built-in gel analysis platform. Protein bands were selected by size and corresponding positive controls and densities used to establish a standard curve for protein mass. Nanoparticle protein content was interpolated from the standard curve (Figure 10A) and calculated for a 20ug CRISPR-AuNP dose.

A.

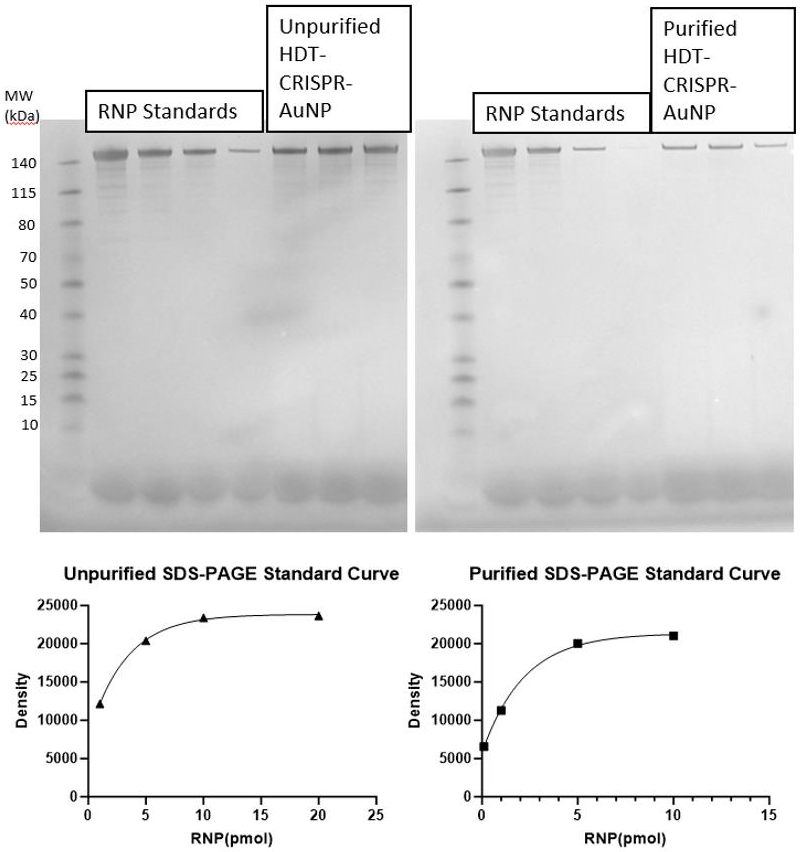
MW (kDa)
RNP Standards
Unpurified HDT-CRISPR-AuNP
RNP Standards
Purified HDT-CRISPR-AuNP
140
115
80
70
50
40
30
25
15
10
Unpurified SDS-PAGE Standard Curve
Density
RNP(pmol)
Purified SDS-PAGE Standard Curve
Density
RNP(pmol)

B.

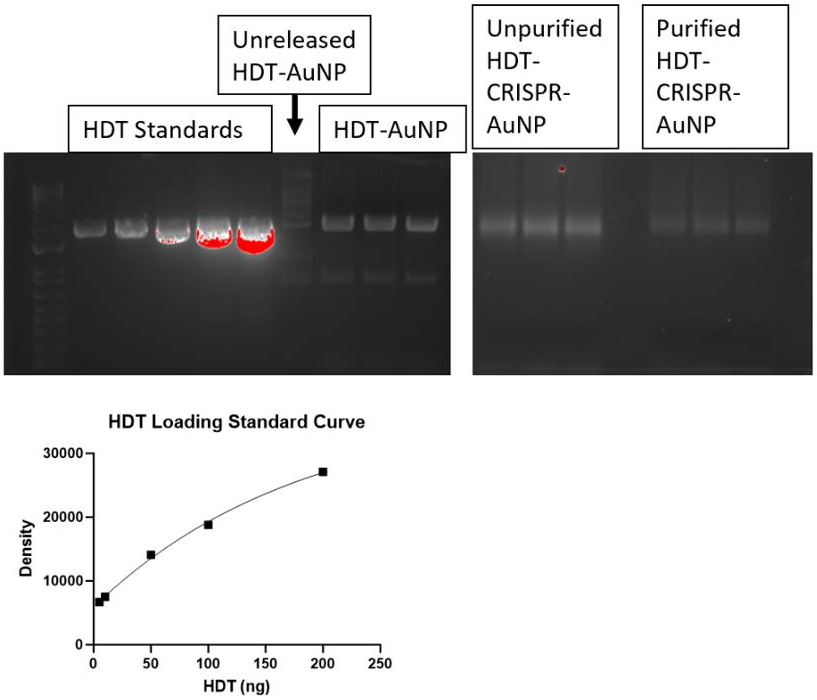
Unreleased HDT-AuNP
HDT Standards
HDT-AuNP
Unpurified HDT-CRISPR-AuNP
Purified HDT-CRISPR-AuNP
HDT Loading Standard Curve
Density
HDT (ng)

Figure 10. HDT-CRISPR-AuNP show Cas9 RNP and HDT loading when analyzed via SDS-PAGE and agarose gel electrophoresis*. (A) Gel images and standard curve for SDS-PAGE analysis of Cas9 RNP loading onto nanoparticle. (B) Agarose gel images and standard curve interpolation for HDT loading onto gold core.*

HDT Loading Characterization by Agarose Gel Electrophoresis

8ug CRISPR-AuNP solution was incubated overnight in 5mM BME to cause release of surface-bound, thiolated nanoparticle cargo. Released nanoparticle solution was combined with 10X BlueJuice gel loading buffer (ThermoFisher) and loaded into an agarose gel for electrophoresis. Samples were run for 45 minutes at 100mV. Bands were analyzed using iBright and a standard curve established for band density. This was used to interpolate nanoparticle DNA content (Figure 10B) and calculated for a 20ug dose.

Jurkat Cell Culture

Jurkat cells (American Type Culture Collection, Manassas, VA, US) were thawed and plated in at 0.5 million cells per mL in Roswell Park Memorial Institute 1640 medium (RPMI, ThermoFisher) with 10% fetal bovine serum (FBS, ThermoFisher) and 1% penicillin streptomycin (ThermoFisher). After two passages in culture, cells were replated in serum-free, antibiotic-free RPMI and serum starved for 2 hours. CRISPR-AuNP or polyplexes were added directly to cell media and incubated for 4 hours before serum addition to media. Electroporated samples were electroporated using a Neon Transfection system according to manufacturer's settings for Jurkat cells (1700mV, 1 pulse, 20ms). Electroporated samples were treated with maximum RNP dose (100pmol RNP) and HDT dose (400ng HDT) and immediately placed into serum-containing

RPMI. After two doubling times (96 hours), cells were harvested for flow cytometry and gene editing analysis.

Primary T Cell Culture:

Primary peripheral blood naïve T cells and primary peripheral blood pan T cells were purchased from STEMCELL Technologies (Vancouver, Canada). For each cell type, four unique donors were sourced, with equal representation of biological sex. Cells were thawed and placed into RPMI supplemented with 5mM BME, 10% FBS (for naïve T cells) or 10% Human AB serum (Sigma-Aldrich) for pan T cells, and 1% penicillin streptomycin, 200 U/mL IL-2, 5ng/mL IL-7, and 5ng/mL IL-15 (ThermoFisher). Cells were plated at 0.5 million cells per 1mL media, rested overnight, and resuspended in 150uL serum-free RPMI 2 hours prior to treatment. After treatment, cells were incubated in serum-free media for an additional 4 hours prior to addition of serum-containing CTL media described above to a final volume of 1mL. Data shown is from unstimulated T cells. Another culture was stimulated with CD3/CD28 Dynabeads 24 hours after nanoparticle treatment, but extremely low viability across all treatment groups resulted in too few live cells for analysis.

CD34+ Cell Culture

Peripheral blood granulocyte colony stimulating factor (GCSF)-mobilized CD34+ blood stem cells were purchased from Core Center of Excellence in Hematology of the Fred Hutchinson Cancer Center (FHCC) following the protocol approved by the Fred Hutch Institutional Review Board (protocol no. 985.03) and in accordance with the Declaration of Helsinki and the Belmont Report. Four unique cell donors were used, with equal representation of biological sex. Cells

were thawed and place into StemSpan™ Serum-Free Expansion Medium version II (StemSpan SFEM II; STEMCELL Technologies) supplemented with 100ng/mL human recombinant stem cell factor (SCF), flightless 3 ligand (flt3-L), and thrombopoietin (TPO). Cells were rested overnight before being replated into non-supplemented Iscove's Modified Dulbecco's Medium (IMDM, ThermoFisher) for 2 hours prior to treatment. Electroporated samples were electroporated according to the manufacturer's instructions (1600mV, 10ms, 1 pulse) and placed immediately into serum-supplemented stem cell media. Nanoparticle and polyplex samples were treated after 2 hours of serum starvation and allowed to incubate for an additional 4 hours. At 4 hours, cells were supplemented with complete media containing SCF, flt3-L and TPO and allowed to incubate a further 4 days (two or more cell doublings) before harvest for gene editing analysis.

Cell Viability Measures

Cell viability was measured using trypan blue dye exclusion assay analyzed on a Countess Automated Cell Counter (Invitrogen). Cell samples were combined 1:1 with Trypan Blue (Invitrogen) prior to automated counting per manufacturer's instructions.

Confocal Microscopy

HDT-CRISPR-AuNP and HDT-polyplex were synthesized using Cas9 RNP formulated using ATTO550-labeled tracrRNA (IDT). Primary pan T cells were treated with nanoparticles or polyplexes as described previously. Cells were incubated with fluorescently labeled treatments for 4 hours, then stained with CellMask Far Red membrane dye (ThermoFisher) and NucBlue Live Cell nuclear stain (Hoechst 33342, ThermoFisher) according to manufacturer instructions. Cells were resuspended in 50uL 1% FBS in 1X phosphate buffered saline (PBS, ThermoFisher)

and imaged on a Zeiss LSM 780 confocal microscope (Carl Zeiss Microscopy, Oberkochen, Germany). Images were analyzed with Zen Blue (Version: 3.1, ZEISS).

Flow Cytometry

Antibody-fluorophore conjugates used in each flow cytometry experiment are detailed in Table 2. For each experiment, cells to be stained and analyzed were washed twice in 3mL PBS to remove excess polymer and decrease the risk of antibody sequestration. Washed cells were stained with Zombie Near Infrared (Zombie NIR™) live/dead stain (BioLegend) at a 1:500 dilution for 15 minutes and washed by centrifugation. For primary naïve and pan T cells, human FcR block (Miltenyi Biotec, Bergisch Gladbach, Germany) was incubated with cells according to manufacturer' instructions for 15 minutes. Cells were washed and resuspended in FACS buffer (2% FBS in PBS) with the antibody cocktail detailed in Table 2 for 45 minutes prior to final wash and acquisition. Cells were acquired on a BD FACSCelesta flow cytometer (BD Biosciences, Franklin Lakes, NJ, US).

Antibody	Clone	Fluorochrome	Dilution
B2M	2M2	PE	1:20
CD3	UCHT1	AF700	1:25
CD4	RPA-T4	V450	1:25
CD8	RPA-T8	APC	1:20
TCRab	IP26	PerCP-Cy5.5	1:20

Table 2. Fluorophore-conjugated antibodies and their dilutions used in flow cytometry studies.

gDNA Extraction and Sequencing

Genomic DNA (gDNA) was extracted from cell samples using the Invitrogen Purelink Genomic DNA Isolation kit (ThermoFisher) according to manufacturer's instructions. For MiSeq analysis of target cut sites, gDNA was amplified using MiSeq adapter primers designed in house for either the human *B2M* or *TRAC* locus (Table 1) according to genome assembly GRCh37. Amplicons

were indexed and multiplexed using Nextera XT v2 indices (Illumina, San Diego, CA, US) and combined into sequencing libraries. Libraries were sequenced using paired end MiSeq. Resulting reads were analyzed for total gene editing and insertion/deletion mutations using an established in house analysis pipeline [132].

Confirmation of Template Insertion by PCR

PCR primers were designed such that the forward primer bound ~150bp upstream of the *TRAC* transgene HDT construct and the reverse primer within the variable β chain of the transgenic TCR such that any product produced would have a size of 645bp. 20ng gDNA per sample was used in each PCR reaction with NEB Q5 HotStart 2x Mastermix (New England BioLabs, Ipswich, MA, US) according for manufacturer's protocol. gDNA samples subjected to this PCR that yielded the expected band were subject to Sanger sequencing using the same forward primer to confirm band identity.

Statistics and Data Reporting

Graphpad Prism (10.0.4; Boston, Ma, USA) was used to present all results as the mean ± SEM. All statistical analyses were performed as Brown-Forsythe and Welch ANOVA tests. Statistical significance was defined as $P \leq 0.05$.

Chapter 3: Discussion

Conclusions:

There is a serious unmet need for inexpensive gene therapy delivery solutions that enable research and development across broad environments. HDT-CRISPR-AuNP is able to deliver both active CRISPR Cas9 RNP and long transgene-encoding DNA cassettes without the need for production of viral vectors, engineered nucleases, or custom lipid or peptide formulations. In this way, HDT-CRISPR-AuNP avoids some of the cost-related pitfalls that are associated with various viral, LNP, eVLP, and peptide-based delivery systems—though it must be noted that these reductions in price come, at present, with lower than desired efficacy. With some established gene therapies able to generate more than 90% [120] editing in vitro, it must be considered that serious further optimization is needed before HDT-CRISPR-AuNP is competitive in the field. While HDT-CRISPR-AuNP as currently dosed has an acceptable effect on cell viability, increasing the dose of both RNP and HDT may increase editing as seen in other gene delivery platforms that deliver upwards of 100pmol RNP per dose [145]. However, large quantities of RNP and peptides used for delivery have been shown to cause significant drops in viability in some cases [145]. Balancing the extent of desirable gene editing with cell viability is a delicate process that must be optimized before any gene therapy can be considered for the clinic. Still, at this point HDT-CRISPR-AuNP is the only fully synthetic nanoparticle-based platform that is capable of delivering transgenes longer than 2kb in length alongside CRISPR cargo all in the same nanoparticle to primary human blood cells. Given that several currently approved gene therapies—including many CAR-T treatments currently performed ex vivo—rely on the inclusion

of long transgenes [19, 69, 79], the successful transition of HDT-CRISPR-AuNP to in vivo circumstances could be transformative to research and healthcare in areas that lack access to electroporation equipment.

While HDT-CRISPR-AuNP demonstrated evident and sometimes statistically significant expression of the GFP reporter transgene from the *B2M* locus, as of this writing, we were not able to validate protein expression of an antigen-specific TCR from the *TRAC* locus. PCR results showed evidence of successful HDR that is unlikely to be spurious, given that the primer located within the transgene is in a recombined sequence that is not present in either unedited T cells or undifferentiated HSPC [150]. It may be the case that HDR was so infrequent that only a few cells expressed the TCR at all, and those were not among the events analyzed by flow cytometry. Conversely, lack of TCR expression was fully expected from HSPC. Editing stem cells rather than mature T cells has potential for life-long antigen-specific lymphocyte production from long-term reconstituting hematopoietic stem cells, which retain stemness throughout the life of the patient while producing differentiating daughter cells. Engineering immunity towards cancer antigens like NY-ESO-1 by editing the stem cell niche may abrogate the need for multiple infusions of ex vivo engineered cell therapies by creating a self-renewing antigen-specific T cell reservoir within the patient's bone marrow.

However, for full confidence in this approach, expression of the engineered TCR must be shown in T cells. Future studies will involve repeating the NY-ESO-1 TRAC nanoparticle study with an analogous dextramer to the one previously used to put to rest questions of faulty dextramer binding. From the data presented herein, HDT-CRISPR-AuNP successfully mediates gene editing

at two candidate loci in T cells, resulting in expression of a reporter transgene and at least integration of a therapeutically relevant TCR construct.

Future Directions:

In addition to repeating the T cell study described above for the purpose of gaining clarity on TCR transgene expression in vitro, there are multiple exciting avenues to explore with HDT-CRISPR-AuNP. As previously mentioned, transgenes for T cell engineering are often 2kb or shorter [69], meaning that HDT-CRISPR-AuNP could have efficacy as a tool for ex vivo or in vivo generation of CAR-T or TCR-T cell therapies. HDT-CRISPR-AuNP has not yet been probed for the maximum transgene length it can stably load and may be able to load longer dsDNA sequences. While ssDNA HDT is a consideration, the time and expense it takes to produce, as well as stability concerns, secondary structures and self-complementarity causing instability at the HDT-AuNP stage are potential issues.

Still, there are many therapeutic genes that are closer to 2kb and can be delivered as dsDNA. Some engineered monoclonal antibody constructs are 2.5kb or less in length [79], meaning HDT-CRISPR-AuNP could be used to generate antigen-specific B cells or create a stem cell population that differentiates to form B cells with pre-programmed B cell receptors. These technologies both have potential applications in the treatment of cancer and autoimmune disease, as well as HIV [69, 143]. In both T cell and B cell engineering, there is a distinct risk of engineered cells maintaining one unaltered allele that could express natural TCR or antibody chains, resulting in mispairing of engineered TCR or antibody chains with native ones. Roth et al. found that when inserting the same NY-ESO-1 TCR construct into T cells, four possible TCRs

were expressed by edited cells-edited TCRa + edited TCRb, edited TCRa + endogenous TCRb, endogenous TCRa + edited TCRb, and endogenous TCRa + endogenous TCRb [69]. If these native sequences are self-reactive, this could result in potential autoimmunity , as has been observed in prior TCR engineering studies [151]. In this circumstance, it may be a benefit to have higher rates of TCR knockout than HDR as seen in T cells edited with HDT-CRISPR-AuNP. Alternately, further modifications, such as the introduction of sequences coding for disulfide bonds, can be made to the template DNA itself to ensure close physical proximity and binding of the edited TCR components [152].

Additionally, further optimization to increase transgene integration efficacy could abrogate the need for knockout altogether. When considering the three key steps of the process of gene editing--(1) cellular entry of all cargo, (2) nuclear trafficking of genome engineering cargo, and (3) gene editing at the desired locus, each step can be targeted for improved activity. Many different endocytosis pathways exist, and which is used to take up a nanoparticle in solution is dependent on cell type, cell state, and culture conditions [153]. Quiescent cell types such as HSPC are more likely to engage in passive pinocytosis, an endocytic pathway wherein cells passively sample their environment to gauge whether or not to start cellular processes such as differentiation [154]. This is also a preferred pathway for naïve lymphocytes, which await environment signals directing such processes as activation and division [155].

Investigating alternate polymers and copolymers may also yield better cellular entry and endosomal escape results. While heavy PEGylation appears to be necessary in our PEI-based system to mitigate toxicity while increasing uptake, other polymers such as poly(lactic-co-glycolic acid) (PLGA) and poly(beta-amino esters)(PBAE) have also been shown to be capable of

endosomal escape[156, 157], and to be amenable to thiol modification [158]. Whether these materials are able to form monostable nanoparticles when formulated with HDT-AuNP remains to be evaluated.

Given that HDT-CRISPR-AuNP can carry multiple cargo types, it may be possible to further decorate the particle with cell-penetrating peptides that aid in endosomal escape [159]. Including peptides such as TAT as either thiolated, surface-bound moieties, or covalently bound to the nuclease [145] itself may increase the degree of gene editing cargo introduced into the cell cytoplasm.

In addition to optimizing cellular entry and endosomal escape, nuclear localization could be improved. Our current system relies on two nuclear localization signals (NLS) conjugated to the Cas9 protein. Other groups have shown that increasing the number of NLS domains or including alternate NLS peptides can increase gene editing mediated by Cas9 [160, 161].

Lastly, increasing the efficiency of the gene editing cargo itself can help maximize editing at the target locus. With novel CRISPR systems being developed at increasing speeds, there are many possible gene editing systems which could promote higher levels of target transgene integration. Further optimization could involve replacing Cas9 with more efficient engineered nucleases, such as iGeoCas9 [127], or abandoning DSB-inducing CRISPR systems for technologies such as eePASSIGE or CAST [55, 56]. These systems rely on codelivery of engineered bacterial recombinases and transposes, respectively, with primer editors and DNA templates in the form of plasmids to mediate large gene integrations without the need for DSBs [55]. Removing DSBs from the gene insertion process may mitigate potentially genotoxic

downstream effects of off-target cutting, and may allow for more efficient gene insertion than relying on the cell's endogenous HDR machinery. However, whether loading this tripartite cargo onto an AuNP core will result in monostable particles of acceptable size remains to be seen. If all components are easily thiolated without damaging protein activity, and if they are easily formulated into a polyplex with PEI-PEG or other optimized polymers, eePASSIGE and CAST systems may synergize well with HDT-CRISPR-AuNP.

Of course, as noted earlier in this thesis, the possibility for in vivo administration of a synthetic nanoparticle to deliver gene editing to target cells with therapeutic efficacy and safety is a key goal for the field. In the described studies, purified cells were treated ex vivo in serum-free conditions. In vivo, nanoparticles will be subjected to not only physiologic conditions, but depending on the route of administration, physical stress as well. Administration of a nanoparticle solution via syringe necessarily involves shear stress, the effects of which have not been evaluated on HDT-CRISPR-AuNP. Further, nanoparticles have thus far been formulated and stored in DNA Lo-Bind and Protein Lo-Bind tubes, which prevent adhesion of the polymer, protein, and nucleic acid components of the particles to the tube walls. The material composition of tools used for injection must be considered from a stability standpoint.

Beyond administration, nanoparticles delivered into the blood stream face an environment very different from in vitro conditions. The peripheral blood contains between 3.5 and 5.5g/dL serum albumin [162], representing a much higher serum content than even serum-supplemented media. These peripheral blood proteins are likely to interact with the cationic polymer corona of the nanoparticle and may represent a significant barrier in uptake into circulating cells [163].

Overall Conclusions:

The promise of gene therapy to transform human health is dependent on the ability to deliver genetic engineering with safety and efficacy. Here we describe a proof-of-concept synthetic nanoparticle that can deliver active CRISPR Cas9 RNP cargo alongside a long, dsDNA template to introduce a new transgene at a target genetic locus in primary human lymphocytes. While efficacy was low with this particle, delivery was substantiated at two different genetic loci. This particle is cost effective and simple to synthesize with commercially available materials and standard laboratory methods, making further development feasible for many different laboratory settings. The ability to use volume-fill estimation for cargo loading and to swap out different polymeric or CRISPR system cargo without the need for complex engineering will greatly accelerate optimization. There are many diseases for which very low levels of transgene delivery can have therapeutic value, especially those setting in which transgene expression is associated with selective expansion of genetically engineered cells. For other disease settings where higher levels of transgene delivery are required for therapeutic efficacy to be achieved, further optimization of HDT-CRISPR-AuNP is needed. For clinical translation of HDT-CRISPR-AuNP, preclinical evaluation in relevant animal models will be an important step to facilitate early regulatory assessment.

Appendix:

Nanoformulation Optimization & In Vivo Studies

Two CRISPR-loaded gold nanoparticle-based gene therapy platforms developed by the Adair Lab preceded HDT-CRISPR-AuNP. The first (1st generation CRISPR-AuNP) was developed by Dr. Reza Shahbazi and is detailed in the lab's 2019 *Nature Materials* paper [132]. This nanoparticle was comprised of a gold core also produced by the Turkevich method of citrate reduction, which was then incubated under highly acidic conditions (pH 3) with an excess of thiol-OEG-modified gRNA (Figure A1A). This allowed complete coating of the AuNP surface with RNA, which was then washed twice prior to incubation with Cas9 or Cas12a nuclease to form RNP on the core surface. This negatively charged RNP-AuNP was then coated in 2000MW branched PEI to achieve a cationic charge. This nanoparticle, as published, could carry short (<100bp) ssHDT molecules bound electrostatically to the polymer layer and achieve HDR in vitro when used to treat human HSPC. Further development of this nanoparticle found that it could also be decorated with electrostatically-bound long ssDNa and dsDNA templates at a ratio of 1ug HDT per 10ug AuNP (Figure A1B). These nanoparticles were loaded with a GFP reporter template as previously described (though targeted to the immunoglobulin heavy chain IGH locus) and were used to treat HSPC in vitro, resulting in good viability but very little gene editing, even with up to five times the AuNP dose than the 20ug demonstrating efficacy in this thesis. These nanoparticles were also unable to induce GFP expression from HSPC in vitro (Figure A1C).

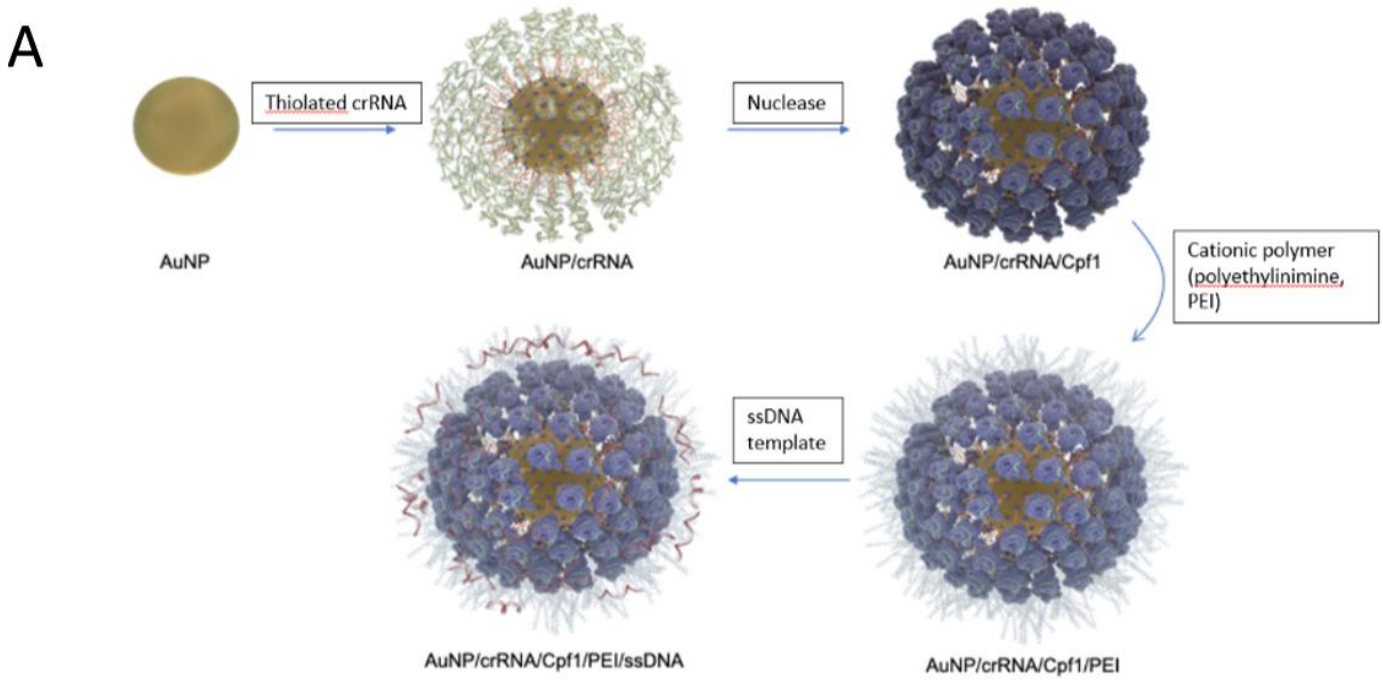
A
Thiolated crRNA
Nuclease
AuNP
AuNP/crRNA
AuNP/crRNA/Cpf1
Cationic polymer (polyethylinimine, PEI)
ssDNA template
AuNP/crRNA/Cpf1/PEI/ssDNA
AuNP/crRNA/Cpf1/PEI

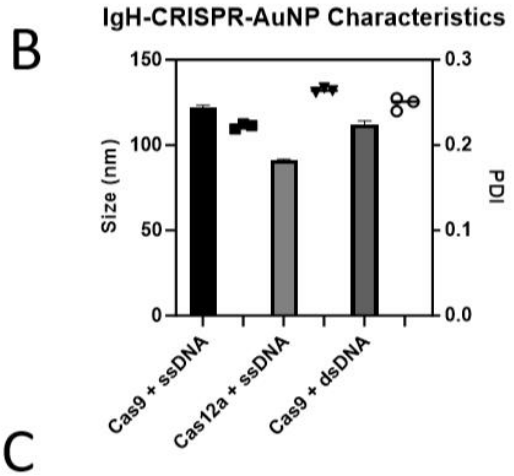
B
IgH-CRISPR-AuNP Characteristics
Size (nm)
PDI
150
100
50
0
0.3
0.2
0.1
0.0
Cas9 + ssDNA
Cas12a + ssDNA
Cas9 + dsDNA

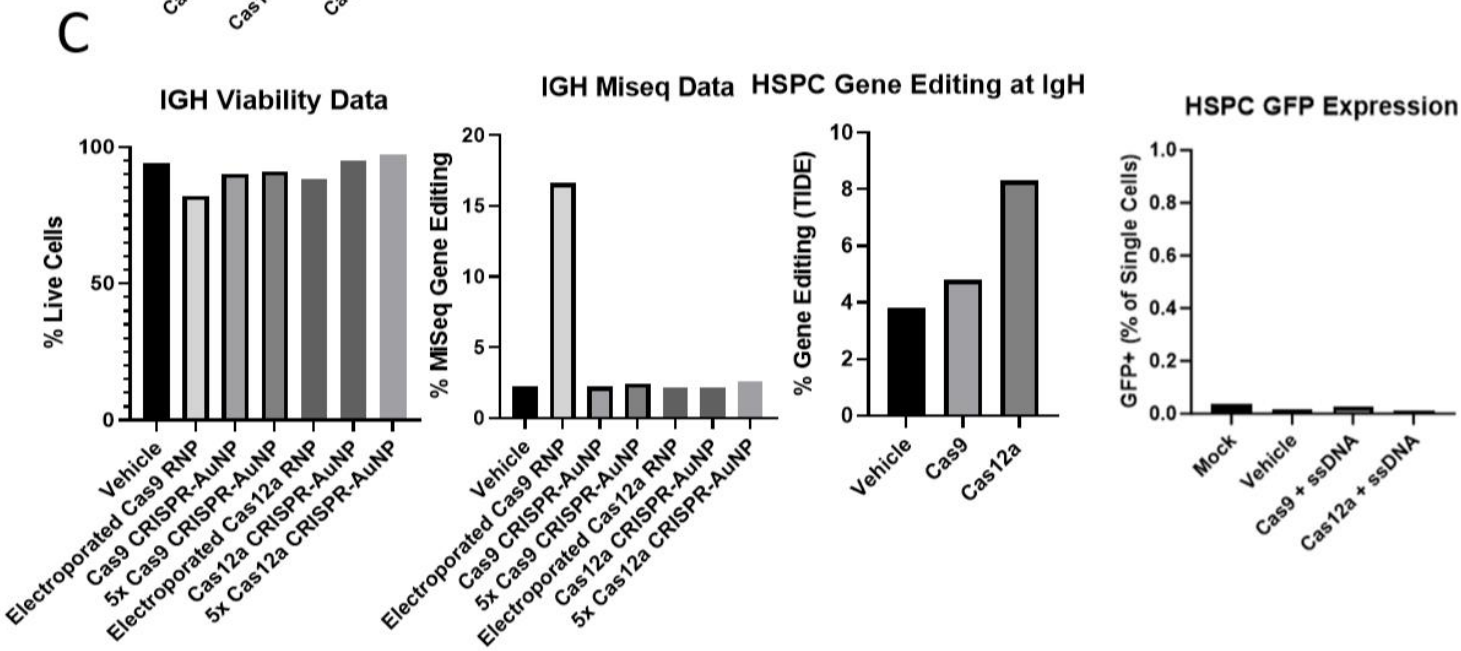
C
IGH Viability Data
% Live Cells
IGH Miseq Data
% MiSeq Gene Editing
HSPC Gene Editing at IgH
% Gene Editing (TIDE)
HSPC GFP Expression
GFP+ (% of Single Cells)
Vehicle
Electroporated Cas9 RNP
Cas9 CRISPR-AuNP
5x Cas9 CRISPR-AuNP
Electroporated Cas12a RNP
Cas12a CRISPR-AuNP
5x Cas12a CRISPR-AuNP
Cas9
Cas12a
Mock
Cas9 + ssDNA
Cas12a + ssDNA

Figure A1. 1st generation CRISPR-AuNP can be stably formulated with long HDT, but show little efficacy in CD34+ cells in vitro. *(A) Synthesis of 1st generation CRISPR-AuNP. (B) DLS analysis showing 1st generation CRISPR-AuNP formulated with long ssDNA and dsDNA. Data represent three technical replicates (dots) as means (gray bars) ± standard error of the mean (error bars). (C) Viability, gene editing data by MiSeq and TIDE (tracking of indels by decomposition) and GFP transgene analsysi by flow cytometry. Data represent one technical replicate per group.*

Nevertheless, we sought to determine whether nanoparticles loaded with Cas9 or Cas12a and a short ssHDT were capable of mediating gene editing and HDR at the IGH locus when delivered to blood stem cells in humanized mice (Figure A2A). While intravenous administration is the least invasive method for in vivo delivery to blood cells, target HSPC are rarely found in circulation. The bone marrow is considered the primary HSPC niche after birth, while liver and spleen can serve as extramedullary niches for HSPC and hematopoiesis, particularly in mice [164]. Intra-bone marrow injection is a possible route of administration to directly access HSPC in their native niche. We first sacrificed five adult humanized NOD-SCID-IL-2γ-null (NSG) mice engrafted as neonates with human CD34+ HSPC and examined single cell suspensions from candidate organs to determine which displayed the highest proportions of CD34+ human cells. We found that the bone marrow of the iliac crest contained the highest frequency and absolute number of human CD34+ cells (Figure A2B). Unfortunately, the iliac crest in mice is fragile and nearly possible to inject in living animals. The second highest population of human CD34+ HSPC was observed in the bone marrow of the femur, which is accessible via injection [165]. Thus, for initial studies we elected to administer nanoparticles via intraosseous injection into one or both femurs.

We injected mice with single dose of 1.5mg/kg (based on gold mass) of either Cas9 or Cas12a loaded nanoparticles carrying a 188bp ssHDT encoding a *NotI* restriction enzyme site as reported in the 2019 Nature Materials paper and analyzed peripheral blood biweekly for indels and lymphocyte development. Mice showed no evidence for acute toxicity post-injection, as determined by continuous weight gain (Figure A2C). However, indel frequency as measured by Sanger sequencing did not meet statistical significance, and revealed that Cas9 was largely inactive on this nanoparticle (Figure A2D). This observation was confirmed and expounded upon in a 2024 publication headed by Dr. Daniel Lane, which found that a combination of steric hindrance and instability of the duplex gRNA at pH of 3 resulted little to no active Cas9 loading onto the 1st generation CRISPR-AuNP and no detectable Cas9 RNP activity in an in-tube DNA cutting assay which I developed [102].

A

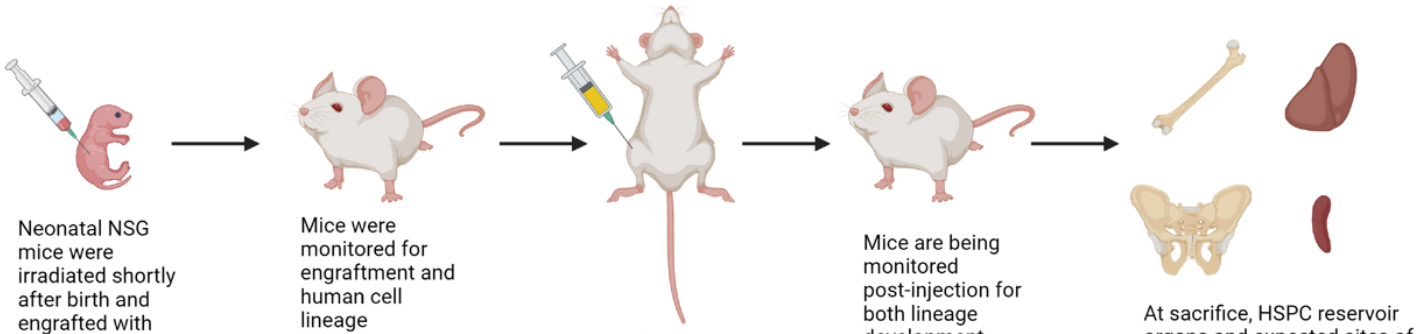
Neonatal NSG mice were irradiated shortly after birth and engrafted with cord-blood derived CD34+ human HSPC
Mice were monitored for engraftment and human cell lineage development in peripheral blood via flow cytometry
At 15 weeks of age, mice were injected intraosseously with 1.5mg/kg IGH-CRISPR-AuNP.
Mice are being monitored post-injection for both lineage development and gene editing in peripheral blood.
At sacrifice, HSPC reservoir organs and expected sites of nanoparticle aggregation will be analyzed for gene editing.

B

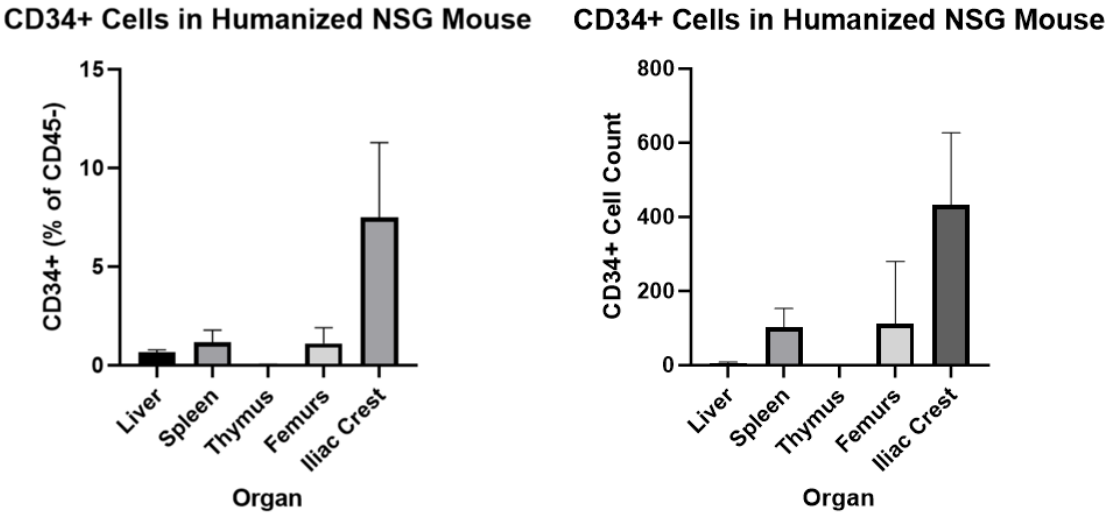
CD34+ Cells in Humanized NSG Mouse
CD34+ (% of CD45-)
15
10
5
0
Liver
Spleen
Thymus
Femurs
Iliac Crest
Organ
CD34+ Cells in Humanized NSG Mouse
CD34+ Cell Count
800
600
400
200
0
Liver
Spleen
Thymus
Femurs
Iliac Crest
Organ

C

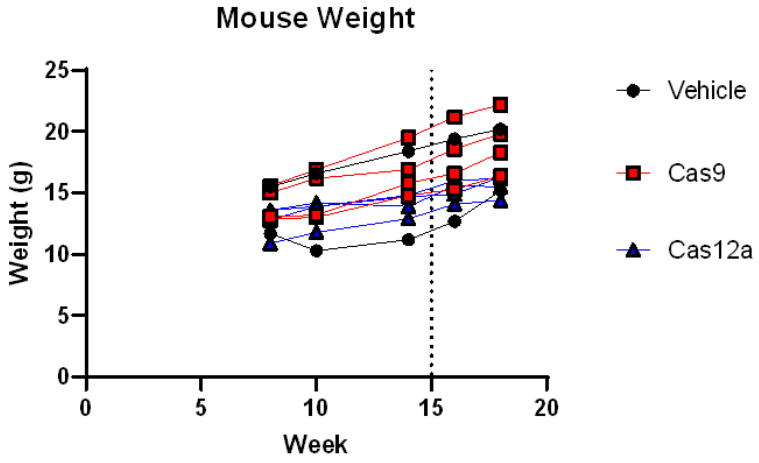
Mouse Weight
Weight (g)
25
20
15
10
5
0
0
5
10
15
20
Week
Vehicle
Cas9
Cas12a

D

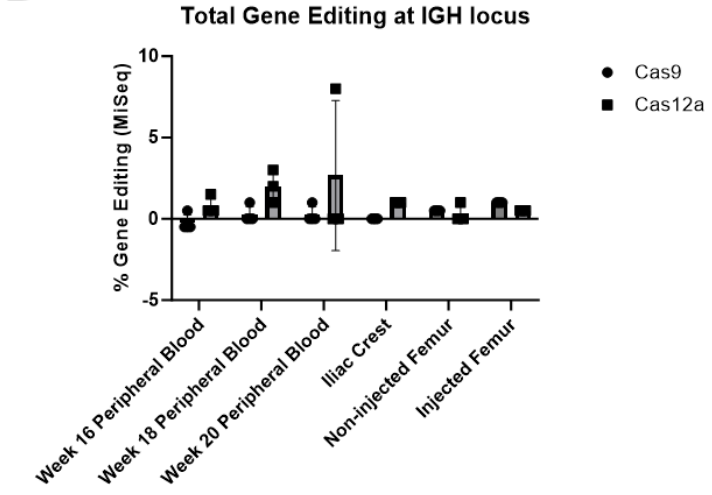
Total Gene Editing at IGH locus
% Gene Editing (MiSeq)
10
5
0
-5
Week 16 Peripheral Blood
Week 18 Peripheral Blood
Week 20 Peripheral Blood
Iliac Crest
Non-injected Femur
Injected Femur
Cas9
Cas12a

Figure A2. Humanized NSG mice injected intrafemorally with 1st generation HDT-CRISPR-AuNP show no acute toxicity but limited gene editing. *(A) Schematic for treatment of humanized NSG mice with 1st generation HDT-CRISPR-AuNP. (B) Flow cytometry analysis of single-cell suspensions derived from murine tissues. Data represent five biological replicates as means (gray bars) ± standard error of the mean (error bars). C. Mouse weight over time relatively to nanoparticle injection. Data represent four biological replicates for Cas9 and Cas12a groups, and two biological replicates for vehicle mice. D. Gene editing analysis by Miseq for peripheral blood and bone marrow of treated mice. Data represent four biological replicates (dots) as means (gray bars) ± standard error of the mean (error bars).*

This discovery led to the development of the 2nd generation CRISPR-AuNP also detailed in Lane et. al. 2nd generation CRISPR-AuNP are formulated using the same gold nanoparticle cores but incubating a preformed RNP complex with the AuNP at a slightly less acidic pH of 3.8 determined to be optimal by physiochemical analysis (Figure A3A). Notably, this nanoparticle was not stable with 2kMW branched PEI, necessitating the use of a PEI copolymer grafted with 10% thiolated polyethylene glycol (2k-g10-PEI-PEG-SH) [lane et al]. This nanoparticle was amenable to electrostatic decoration with dsHDT, as evidenced by clinically viable and monostable characteristics as measured by DLS when formulated with Cas12a RNP and a 2.1kb HDT encoding a GFP reporter transgene targeted for the human IGH locus (Figure A3B). This nanoparticle formulation was compared with 1st generation CRISPR-AuNP with the same RNP and HDT in vivo in humanized NSG mice (Figure A3C). Mice were given three CRISPR-AuNP injections at a dose of 1.5mg/kg (based on gold mass) and monitored for acute toxicity and gene editing. Flow cytometry was performed to detect GFP expression in peripheral blood.

While peripheral blood demonstrated indels at IGH and some GFP expression, levels did not reach statistical significance before the end of the study (Figure A3D). Importantly, no significant GFP expression was observed following treatment with either 1st or 2nd generation CRISPR-AuNP. The findings from these in vivo studies were pivotal in providing the basis for the 3rd generation CRISPR-AuNP upon which HDT-CRISPR-AuNP is based.

A

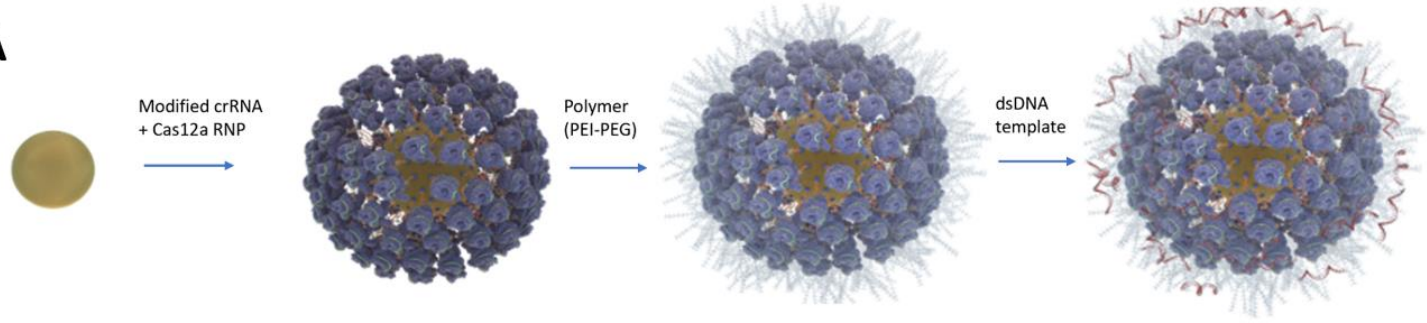

B

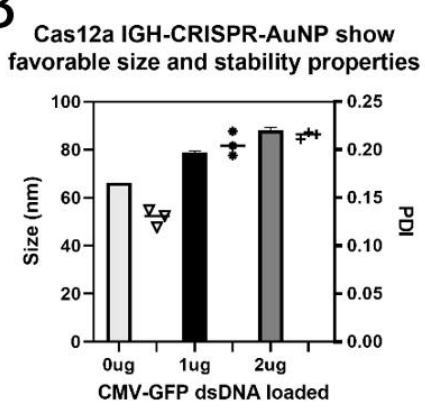

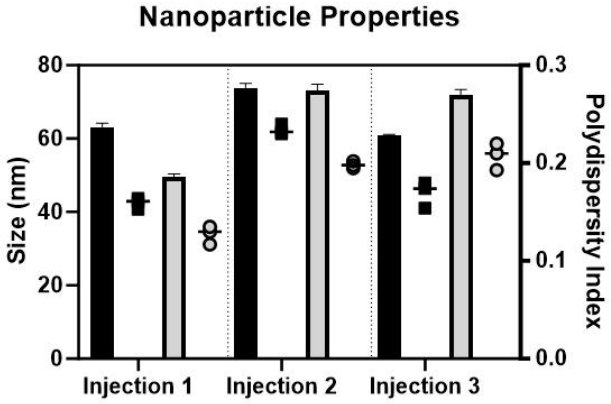

C

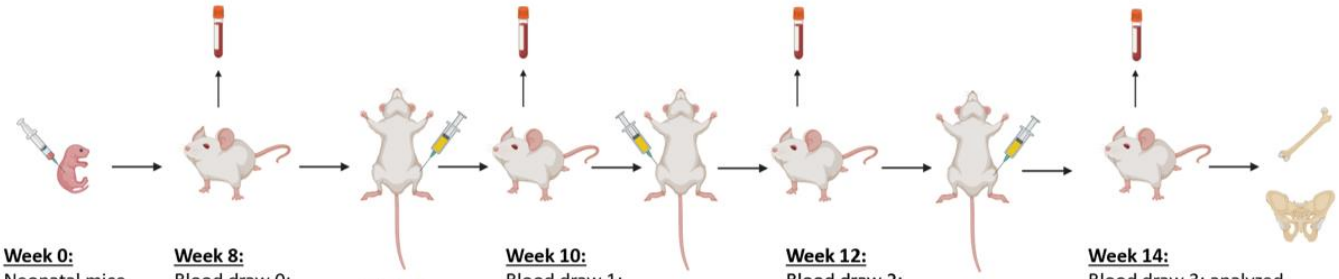

Week 0: Neonatal mice engrafted with human CD34+cord blood cells

Week 8: Blood draw 0: analyzed for lineage development and human cell engraftment

Week 9: CRISPR-AuNP injection 1 (Right femur)

Week 10: Blood draw 1: analyzed for lineage development, engraftment, and GFP expression. gDNA saved for analysis.

Week 11: CRISPR-AuNP injection 2 (Left femur)

Week 12: Blood draw 2: analyzed for lineage development, engraftment, and GFP expression. gDNA saved for analysis.

Week 13: CRISPR-AuNP injection 3 (Right femur)

Week 14: Blood draw 3: analyzed for lineage development, engraftment, and GFP expression.

Organs: Single cell suspensions generated for B cell and GFP analysis via flow and gDNA

D

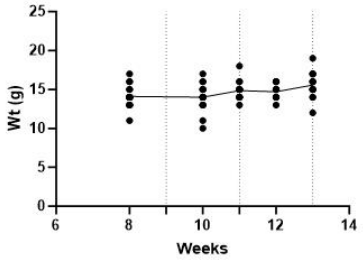

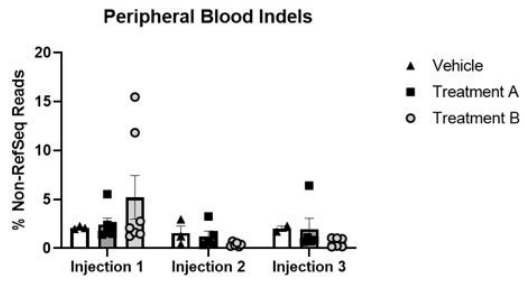

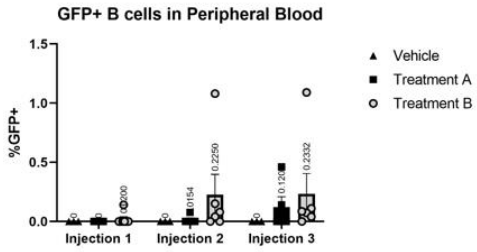

Figure A3. Comparing 1st and 2nd generation HDT-CRISPR-AuNP administration to humanized mice showed better but still insufficient performance of 2nd generation nanoparticle. (A) *Synthesis schematic for 2nd generation HDT-CRISPR-AuNP. (B) DLS analysis showing 2nd generation HDT-CRISPR-AuNP formulated with long dsDNA (left) and DLS data for each nanoparticle formulation injected into mice, where Treatment A is 1st generation and Treatment B is 2nd generation. Data represent three technical replicates (dots) as means (gray bars) ± standard error of the mean (error bars).* (C) Schematic of 1st generation and 2nd generation HDT-CRISPR-AuNP comparison in humanized NSG mice. (D) Analysis of toxicity by weight loss (left), gene editing at IGH by peripheral blood indels (middle) and transgene expression in peripheral blood (right). Data represent seven biological replicates for nanoparticle-treated groups and three biological replicates for vehicle-treated mice.

Acknowledgements

I would like to thank Jennifer E. Adair, Karthikeya Gottimukkala, Daniel Lane, Katrina Poljakov, Trisha Lipson, Jack Castelli, Molly Cassidy, Alessandro Rizzi, Rachel Kyeyune, Haleema Sadia Malik, and Grady Gastelum for support. Research reported in this thesis was supported by the National Institutes of Health Office of the Director, Office of Research Infrastructure Programs (ORIP) under award number P51OD010425 and U42OD011123. The content is solely the responsibility of the authors and does not necessarily represent the official views of the National Institutes of Health. This research was supported by the Genomics and Bioinformatics Shared Resource, the Scientific Imaging Shared Resource, and the Flow Cytometry Shared Resource of the Fred Hutch/University of Washington/Seattle Children's Cancer Consortium (P30 CA015704). This study was supported by NIH grants R01AI158728 and R01AI167009 (MPIs: J. Adair and J. Taylor), T32 GM095421-10 and TL1 TR002318 (both awarded to trainee R. Cunningham), by a grant from the Bill and Melinda Gates Foundation (INV002613; PI J. Adair), and the Fred Hutchinson Cancer Center Evergreen Fund. J. Adair received support as The Fleischauer Family Endowed Chair in Gene Therapy Translation.

In addition, I would like to thank all the members current and former of the Adair Lab, the students and administrators of the University of Washington's Molecular Medicine and Mechanisms of Disease PhD program, and the members of my supervisory committee, without whose support this thesis would not have been possible.

References

[1] Chancellor, D., Barrett, D., Nguyen-Jatkoe, L., Millington, S. & Eckhardt, F. The state of cell and gene therapy in 2023. *Mol Ther* **31**, 3376–3388 (2023).

[2] Shukla, V., Seoane-Vazquez, E., Fawaz, S., Brown, L. & Rodriguez-Monguio, R. The Landscape of Cellular and Gene Therapy Products: Authorization, Discontinuations, and Cost. *Human Gene Therapy Clinical Development* **30**, 102–113 (2019).

[3] Kaji, E. H. & Leiden, J. M. Gene and Stem Cell Therapies. *JAMA* **285**, 545–550 (2001).

[4] Ramirez-Phillips, A. C. & Liu, D. Therapeutic Genome Editing and In Vivo Delivery. *AAPS J* **23**, 80 (2021).

[5] Gonçalves, G. A. R. & Paiva, R. de M. A. Gene therapy: advances, challenges and perspectives. *Einstein (Sao Paulo)* **15**, 369–375 (2017).

[6] Keeler, A. M., ElMallah, M. K. & Flotte, T. R. Gene Therapy 2017: Progress and Future Directions. *Clin Transl Sci* **10**, 242–248 (2017).

[7] Naam, R. 'More Than Human'. *The New York Times* (2005).

[8] Sibbald, B. Death but one unintended consequence of gene-therapy trial. *CMAJ* **164**, 1612 (2001).

[9] Smaglik, P. Clinical trials end at gene-therapy institute…. *Nature* **405**, 497–497 (2000).

[10] Hacein-Bey-Abina, S. *et al.* LMO2-associated clonal T cell proliferation in two patients after gene therapy for SCID-X1. *Science* **302**, 415–419 (2003).

[11] Howe, S. J. *et al.* Insertional mutagenesis combined with acquired somatic mutations causes leukemogenesis following gene therapy of SCID-X1 patients. *J Clin Invest* **118**, 3143–3150 (2008).

[12] Hacein-Bey-Abina, S. *et al.* Insertional oncogenesis in 4 patients after retrovirus-mediated gene therapy of SCID-X1. *J Clin Invest* **118**, 3132–3142 (2008).

[13] Hastie, E. & Samulski, R. J. Adeno-Associated Virus at 50: A Golden Anniversary of Discovery, Research, and Gene Therapy Success—A Personal Perspective. *Hum Gene Ther* **26**, 257–265 (2015).

[14] Naldini, L. *et al.* In vivo gene delivery and stable transduction of nondividing cells by a lentiviral vector. *Science* **272**, 263–267 (1996).

[15] Bulcha, J. T., Wang, Y., Ma, H., Tai, P. W. L. & Gao, G. Viral vector platforms within the gene therapy landscape. *Sig Transduct Target Ther* **6**, 1–24 (2021).

[16] LUXTURNA® (voretigene neparvovec-rzyl). *LUXTURNA® (voretigene neparvovec-rzyl)* https://luxturna.com/.

[17] Introduction. in *Clinical Review Report: Voretigene Neparvovec (Luxturna): (Novartis Pharmaceuticals Canada Inc.): Indication: Vision loss, inherited retinal dystrophy [Internet]* (Canadian Agency for Drugs and Technologies in Health, 2021).

[18] Awasthi, R., Maier, H. J., Zhang, J. & Lim, S. Kymriah® (tisagenlecleucel) – An overview of the clinical development journey of the first approved CAR-T therapy. *Hum Vaccin Immunother* **19**, 2210046.

[19] Commissioner, O. of the. FDA approves CAR-T cell therapy to treat adults with certain types of large B-cell lymphoma. *FDA* https://www.fda.gov/news-events/press-announcements/fda-approves-car-t-cell-therapy-treat-adults-certain-types-large-b-cell-lymphoma (2020).

[20] Klug, A. The discovery of zinc fingers and their development for practical applications in gene regulation and genome manipulation. *Q Rev Biophys* **43**, 1–21 (2010).

[21] Urnov, F. D., Rebar, E. J., Holmes, M. C., Zhang, H. S. & Gregory, P. D. Genome editing with engineered zinc finger nucleases. *Nat Rev Genet* **11**, 636–646 (2010).

[22] Khan, S. H. Genome-Editing Technologies: Concept, Pros, and Cons of Various Genome-Editing Techniques and Bioethical Concerns for Clinical Application. *Molecular Therapy Nucleic Acids* **16**, 326–334 (2019).

[23] Pros and cons of ZNFs, TALENs, and CRISPR/Cas. https://www.jax.org/news-and-insights/jax-blog/2014/march/pros-and-cons-of-znfs-talens-and-crispr-cas.

[24] Reik, A. *et al.* Zinc finger nucleases targeting the glucocorticoid receptor allow IL-13 zetakine transgenic CTLs to kill glioblastoma cells in vivo in the presence of immunosuppressing glucocorticoids. *Cancer Research* **68**, 2557 (2008).

[25] Perez, E. E. *et al.* Establishment of HIV-1 resistance in CD4+ T cells by genome editing using zinc-finger nucleases. *Nat Biotechnol* **26**, 808–816 (2008).

[26] Gupta, R. M. & Musunuru, K. Expanding the genetic editing tool kit: ZFNs, TALENs, and CRISPR-Cas9. *J Clin Invest* **124**, 4154–4161 (2014).

[27] Gaj T, Gersbach CA, Barbas CF 3rd. ZFN, TALEN, and CRISPR/Cas-based methods for genome engineering. Trends Biotechnol. 2013 Jul;31(7):397-405. doi: 10.1016/j.tibtech.2013.04.004. Epub 2013 May 9. PMID: 23664777; PMCID: PMC3694601.

[28] Cui, Z. et al. The comparison of ZFNs, TALENs, and SpCas9 by GUIDE-seq in HPV-targeted gene therapy. Molecular Therapy - Nucleic Acids 26, 1466–1478 (2021).

[29] Mussolino, C. *et al.* A novel TALE nuclease scaffold enables high genome editing activity in combination with low toxicity. *Nucleic Acids Res* **39**, 9283–9293 (2011).

[30] Silva, G. *et al.* Meganucleases and Other Tools for Targeted Genome Engineering: Perspectives and Challenges for Gene Therapy. *Curr Gene Ther* **11**, 11–27 (2011).

[31] Daboussi, F., Stoddard, T. J. & Zhang, F. Engineering Meganuclease for Precise Plant Genome Modification. in *Advances in New Technology for Targeted Modification of Plant Genomes* (eds. Zhang, F., Puchta, H. & Thomson, J. G.) 21–38 (Springer, New York, NY, 2015). doi:10.1007/978-1-4939-2556-8_2.

[32] megaTALs: a rare-cleaving nuclease architecture for therapeutic genome engineering | Nucleic Acids Research | Oxford Academic. https://academic.oup.com/nar/article/42/4/2591/2437518.

[33] González Castro, N., Bjelic, J., Malhotra, G., Huang, C. & Alsaffar, S. H. Comparison of the Feasibility, Efficiency, and Safety of Genome Editing Technologies. *Int J Mol Sci* **22**, 10355 (2021).

[34] Bhokisham, N. *et al.* CRISPR-Cas System: The Current and Emerging Translational Landscape. *Cells* **12**, 1103 (2023).

[35] Jinek, M. *et al.* A programmable dual-RNA-guided DNA endonuclease in adaptive bacterial immunity. *Science* **337**, 816–821 (2012).

[36] Frangoul, H. *et al.* Exagamglogene Autotemcel for Severe Sickle Cell Disease. *New England Journal of Medicine* **390**, 1649–1662 (2024).

[37] Ishino, Y., Shinagawa, H., Makino, K., Amemura, M. & Nakata, A. Nucleotide sequence of the iap gene, responsible for alkaline phosphatase isozyme conversion in Escherichia coli, and identification of the gene product. *J Bacteriol* **169**, 5429–5433 (1987).

[38] Mojica, F. J. M., Díez-Villaseñor, C., Soria, E. & Juez, G. Biological significance of a family of regularly spaced repeats in the genomes of Archaea, Bacteria and mitochondria. *Molecular Microbiology* **36**, 244–246 (2000).

[39] Garneau, J. E. *et al.* The CRISPR/Cas bacterial immune system cleaves bacteriophage and plasmid DNA. *Nature* **468**, 67–71 (2010).

[40] Sternberg, S. H., Redding, S., Jinek, M., Greene, E. C. & Doudna, J. A. DNA interrogation by the CRISPR RNA-guided endonuclease Cas9. *Nature* **507**, 62–67 (2014).

[41] Ahle, S. Gene Therapy: The Comeback Kid of Hematology Treatments? *ASH Clinical News* https://www.ashclinicalnews.org/spotlight/feature-articles/gene-therapy-comeback-kid-hematology-treatments/ (2021).

[42] Li, T. et al. CRISPR/Cas9 therapeutics: progress and prospects. Sig Transduct Target Ther 8, 1–23 (2023).

[43] Asmamaw, M. & Zawdie, B. Mechanism and Applications of CRISPR/Cas-9-Mediated Genome Editing. *Biologics* **15**, 353–361 (2021).

[44] Chang, H. H. Y., Pannunzio, N. R., Adachi, N. & Lieber, M. R. Non-homologous DNA end joining and alternative pathways to double-strand break repair. *Nat Rev Mol Cell Biol* **18**, 495–506 (2017).

[45] Yao, X. *et al.* Homology-mediated end joining-based targeted integration using CRISPR/Cas9. *Cell Res* **27**, 801–814 (2017).

[46] Sfeir, A. & Symington, L. S. Microhomology-mediated end joining: a back-up survival mechanism or dedicated pathway? *Trends Biochem Sci* **40**, 701–714 (2015).

[47] Yeh, C. D., Richardson, C. D. & Corn, J. E. Advances in genome editing through control of DNA repair pathways. *Nat Cell Biol* **21**, 1468–1478 (2019).

[48] Liao, H., Wu, J., VanDusen, N. J., Li, Y. & Zheng, Y. CRISPR-Cas9-mediated homology-directed repair for precise gene editing. *Mol Ther Nucleic Acids* **35**, 102344 (2024).

[49] Nambiar, T. S. *et al.* Stimulation of CRISPR-mediated homology-directed repair by an engineered RAD18 variant. *Nat Commun* **10**, 3395 (2019).

[50] Altae-Tran, H. *et al.* Uncovering the functional diversity of rare CRISPR-Cas systems 1 with deep terascale clustering. *MIT News office* (2023).

[51] Lamothe, R. C. *et al.* Novel CRISPR-Associated Gene-Editing Systems Discovered in Metagenomic Samples Enable Efficient and Specific Genome Engineering. *CRISPR J* **6**, 243–260 (2023).

[52] Münch, P. C., Franzosa, E. A., Stecher, B., McHardy, A. C. & Huttenhower, C. Identification of natural CRISPR systems and targets in the human microbiome. *Cell Host Microbe* **29**, 94-106.e4 (2021).

[53] Eghbalsaied, S. *et al.* CRISPR/Cas9-mediated base editors and their prospects for mitochondrial genome engineering. *Gene Ther* **31**, 209–223 (2024).

[54] Scholefield, J. & Harrison, P. T. Prime editing – an update on the field. *Gene Ther* **28**, 396–401 (2021).

[55] Pandey, S. *et al.* Efficient site-specific integration of large genes in mammalian cells via continuously evolved recombinases and prime editing. *Nat. Biomed. Eng* **9**, 22–39 (2025).

[56] Peters, J. E., Makarova, K. S., Shmakov, S. & Koonin, E. V. Recruitment of CRISPR-Cas systems by Tn7-like transposons. *Proceedings of the National Academy of Sciences* **114**, E7358–E7366 (2017).

[57] Frangoul, H. *et al.* CRISPR-Cas9 Gene Editing for Sickle Cell Disease and β-Thalassemia. *New England Journal of Medicine* **384**, 252–260 (2021).

[58] Sickle Cell Disease - What Is Sickle Cell Disease? | NHLBI, NIH. https://www.nhlbi.nih.gov/health/sickle-cell-disease (2024).

[59] Cao, A. & Galanello, R. Beta-thalassemia. *Genet Med* **12**, 61–76 (2010).

[60] CRISPR Clinical Trials: A 2024 Update. *Innovative Genomics Institute (IGI)* https://innovativegenomics.org/news/crispr-clinical-trials-2024/ (2024).

[61] Ginn, S. L., Mandwie, M., Alexander, I. E., Edelstein, M. & Abedi, M. R. Gene therapy clinical trials worldwide to 2023—an update. *The Journal of Gene Medicine* **26**, e3721 (2024).

[62] Doxzen, K. W. *et al.* The translational gap for gene therapies in low- and middle-income countries. *Sci Transl Med* **16**, eadn1902 (2024).

[63] Global disease burden by region. *Our World in Data* https://ourworldindata.org/grapher/disease-burden-by-region.

[64] Cornetta, K. *et al.* Gene therapy access: Global challenges, opportunities, and views from Brazil, South Africa, and India. *Mol Ther* **30**, 2122–2129 (2022).

[65] Harlow, E. M. & Adair, J. E. Make gene therapies more available by manufacturing them in lower-income nations. *Nature* **631**, 502–504 (2024).

[66] Choudhury, A. *et al.* High-depth African genomes inform human migration and health. *Nature* **586**, 741–748 (2020).

[67] Anjos-Afonso, F. & Bonnet, D. Human CD34+ hematopoietic stem cell hierarchy: how far are we with its delineation at the most primitive level? *Blood* **142**, 509–518 (2023).

[68] Legut, M., Dolton, G., Mian, A. A., Ottmann, O. G. & Sewell, A. K. CRISPR-mediated TCR replacement generates superior anticancer transgenic T cells. *Blood* **131**, 311–322 (2018).

[69] Roth, T. L. *et al.* Reprogramming human T cell function and specificity with non-viral genome targeting. *Nature* **559**, 405–409 (2018).

[70] CRISPR Therapeutics AG. *A Long-Term Follow-up Study of Subjects With Malignancies Treated With CRISPR CAR T Cellular Therapies*. https://clinicaltrials.gov/study/NCT06208878 (2024).

[71] Ottaviano, G. *et al.* Phase 1 clinical trial of CRISPR-engineered CAR19 universal T cells for treatment of children with refractory B cell leukemia. *Sci Transl Med* **14**, eabq3010 (2022).

[72] Iyer, S. P. *et al.* Safety and activity of CTX130, a CD70-targeted allogeneic CRISPR-Cas9-engineered CAR T-cell therapy, in patients with relapsed or refractory T-cell malignancies (COBALT-LYM): a single-arm, open-label, phase 1, dose-escalation study. *The Lancet Oncology* **26**, 110–122 (2025).

[73] Rapid manufacturing of non-activated potent CAR T cells | Nature Biomedical Engineering. https://www.nature.com/articles/s41551-021-00842-6.

[74] Grosser, R., Cherkassky, L., Chintala, N. & Adusumilli, P. S. Combination Immunotherapy with CAR T Cells and Checkpoint Blockade for the Treatment of Solid Tumors. *Cancer Cell* **36**, 471–482 (2019).

[75] Liu, W. *A Dose-Escalation Phase I Trial of PD-1 Knockout Engineered T Cells for the Treatment of Castration Resistant Prostate Cancer*. https://clinicaltrials.gov/study/NCT02867345 (2019).

[76] Lu, Y. *A Phase I Clinical Trial of PD-1 Knockout Engineered T Cells Treating Patients With Advanced Non-Small Cell Lung Cancer*. https://clinicaltrials.gov/study/NCT02793856 (2020).

[77] Wu, S. *Safety and Activity of Programmed Cell Death-1 Knockout Engineered T Cells in Patients With Previously Treated Advanced Esophageal Squamous Cell Carcinoma: An Open-Label, Single-Arm Phase 1 Study*. https://clinicaltrials.gov/study/NCT03081715 (2019).

[78] Svane, I. M. *T-Cell Therapy with CRISPR PD1-Edited Tumor Infiltrating Lymphocytes for Patients with Metastatic Melanoma*. https://clinicaltrials.gov/study/NCT06783270 (2025).

[79] Moffett, H. F. *et al.* B cells engineered to express pathogen-specific antibodies protect against infection. *Sci Immunol* **4**, eaax0644 (2019).

[80] Nahmad, A. D. *et al.* In vivo engineered B cells secrete high titers of broadly neutralizing anti-HIV antibodies in mice. *Nat Biotechnol* **40**, 1241–1249 (2022).

[81] Voss, J. E. *et al.* Reprogramming the antigen specificity of B cells using genome-editing technologies. *Elife* **8**, e42995 (2019).

[82] Cheng, R. Y.-H. *et al.* Ex vivo engineered human plasma cells exhibit robust protein secretion and long-term engraftment in vivo. *Nat Commun* **13**, 6110 (2022).

[83] Hartweger, H. *et al.* HIV-specific humoral immune responses by CRISPR/Cas9-edited B cells. *J Exp Med* **216**, 1301–1310 (2019).

[84] Khoshandam, M., Soltaninejad, H., Hamidieh, A. A. & Hosseinkhani, S. CRISPR, CAR-T, and NK: Current applications and future perspectives. *Genes & Diseases* **11**, 101121 (2024).

[85] Marin, D. *et al.* Safety, efficacy and determinants of response of allogeneic CD19-specific CAR-NK cells in CD19+ B cell tumors: a phase 1/2 trial. *Nat Med* **30**, 772–784 (2024).

[86] Chan, W., Gottschalk, R. A., Yao, Y., Pomerantz, J. L. & Germain, R. N. Efficient Immune Cell Genome Engineering with Enhanced CRISPR Editing Tools. *ImmunoHorizons* **5**, 117–132 (2021).

[87] Wellhausen, N., Agarwal, S., Rommel, P. C., Gill, S. I. & June, C. H. Better living through chemistry: CRISPR/Cas engineered T cells for cancer immunotherapy. *Curr Opin Immunol* **74**, 76–84 (2022).

[88] Cliff, E. R. S. *et al.* High Cost of Chimeric Antigen Receptor T-Cells: Challenges and Solutions. *Am Soc Clin Oncol Educ Book* e397912 (2023) doi:10.1200/EDBK_397912.

[89] Rodrigues, M., Duran, E., Eschgfaeller, B., Kuzan, D. & Habucky, K. Optimizing Commercial Manufacturing of Tisagenlecleucel for Patients in the US: A 4-Year Experiential Journey. *Blood* **138**, 1768 (2021).

[90] Ran, T., Eichmüller, S. B., Schmidt, P. & Schlander, M. Cost of decentralized CAR T-cell production in an academic nonprofit setting. *International Journal of Cancer* **147**, 3438–3445 (2020).

[91] Palani, H. K. *et al.* Decentralized manufacturing of anti CD19 CAR-T cells using CliniMACS Prodigy®: real-world experience and cost analysis in India. *Bone Marrow Transplant* **58**, 160–167 (2023).

[92] Carrillo, M. A. *et al.* Stem cell-derived CAR T cells show greater persistence, trafficking, and viral control compared to *ex vivo* transduced CAR T cells. *Molecular Therapy* **32**, 1000–1015 (2024).

[93] Dolnikov, A., Sylvie, S., Xu, N. & O'Brien, T. Stem Cell Approach to Generate Chimeric Antigen Receptor Modified Immune Effector Cells to Treat Cancer. *Blood* **124**, 2437 (2014).

[94] Kitchen, S. G. *et al.* Engineering Antigen-Specific T Cells from Genetically Modified Human Hematopoietic Stem Cells in Immunodeficient Mice. *PLOS ONE* **4**, e8208 (2009).

[95] Gschweng, E. H. *et al.* A Pre-Clinical Model Of Hematopoietic Stem Cell Based Immunotherapy For Cancer Utilizing The NY-ESO-1 T-Cell Receptor and sr39TK PET Reporter / Suicide Gene. *Blood* **122**, 2020 (2013).

[96] Dong, G. *et al.* Stemness-related genes revealed by single-cell profiling of naïve and stimulated human CD34+ cells from CB and mPB. *Clinical and Translational Medicine* **13**, e1175 (2023).

[97] Powers, J. M. & Trobridge, G. D. Identification of Hematopoietic Stem Cell Engraftment Genes in Gene Therapy Studies. *J Stem Cell Res Ther* **2013**, S3:004 (2013).

[98] Pascutti, M. F., Erkelens, M. N. & Nolte, M. A. Impact of Viral Infections on Hematopoiesis: From Beneficial to Detrimental Effects on Bone Marrow Output. *Front Immunol* **7**, 364 (2016).

[99] Thompson, E. N., Carlino, M. J., Scanlon, V. M., Grimes, H. L. & Krause, D. S. Assay optimization for the objective quantification of human multilineage colony-forming units. *Exp Hematol* **124**, 36-44.e3 (2023).

[100] Thompson, E. N., Carlino, M. J., Scanlon, V. M., Grimes, H. L. & Krause, D. S. Assay optimization for the objective quantification of human multilineage colony-forming units. *Exp Hematol* **124**, 36-44.e3 (2023).

[101] Castelli, J. M. P. *et al.* In vivo production of an anti-HIV antibody from primate hematopoietic cells by non-viral knock-in. *bioRxiv* 2025.05.02.651933 (2025) doi:10.1101/2025.05.02.651933.

[102] Logan, A. C., Lutzko, C. & Kohn, D. B. Advances in lentiviral vector design for gene-modification of hematopoietic stem cells. *Curr Opin Biotechnol* **13**, 429–436 (2002).

[103] Naso, M. F., Tomkowicz, B., Perry, W. L. & Strohl, W. R. Adeno-Associated Virus (AAV) as a Vector for Gene Therapy. *BioDrugs* **31**, 317–334 (2017).

[104] Kalidasan, V. *et al.* A guide in lentiviral vector production for hard-to-transfect cells, using cardiac-derived c-kit expressing cells as a model system. *Sci Rep* **11**, 19265 (2021).

[105] Bak, R. O. & Porteus, M. H. CRISPR-Mediated Integration of Large Gene Cassettes Using AAV Donor Vectors. *Cell Reports* **20**, 750–756 (2017).

[106] Zhang, S., Shen, J., Li, D. & Cheng, Y. Strategies in the delivery of Cas9 ribonucleoprotein for CRISPR/Cas9 genome editing. *Theranostics* **11**, 614–648 (2021).

[107] Walther, J. *et al.* Comparative analysis of lipid Nanoparticle-Mediated delivery of CRISPR-Cas9 RNP versus mRNA/sgRNA for gene editing in vitro and in vivo. *Eur J Pharm Biopharm* **196**, 114207 (2024).

[108] Liu, C., Zhang, L., Liu, H. & Cheng, K. Delivery Strategies of the CRISPR-Cas9 Gene-Editing System for Therapeutic Applications. *J Control Release* **266**, 17–26 (2017).

[109] Jamour, P., Jamali, A., Langeroudi, A. G., Sharafabad, B. E. & Abdoli, A. Comparing chemical transfection, electroporation, and lentiviral vector transduction to achieve optimal transfection conditions in the Vero cell line. *BMC Molecular and Cell Biology* **25**, 15 (2024).

[110] Liang, X. *et al.* Rapid and highly efficient mammalian cell engineering via Cas9 protein transfection. *Journal of Biotechnology* **208**, 44–53 (2015).

[111] Arabi, F., Mansouri, V. & Ahmadbeigi, N. Gene therapy clinical trials, where do we go? An overview. *Biomedicine & Pharmacotherapy* **153**, 113324 (2022).

[112] Shirley, J. L., de Jong, Y. P., Terhorst, C. & Herzog, R. W. Immune Responses to Viral Gene Therapy Vectors. *Mol Ther* **28**, 709–722 (2020).

[113] Wang, J.-H., Gessler, D. J., Zhan, W., Gallagher, T. L. & Gao, G. Adeno-associated virus as a delivery vector for gene therapy of human diseases. *Sig Transduct Target Ther* **9**, 1–33 (2024).

[114] Johnson, K. Novel lentiviral vector advances gene therapy for rare neurological disease. *RegMedNet* https://www.regmednet.com/novel-lentiviral-vector-advances-gene-therapy-for-rare-neurological-disease/ (2025).

[115] Kingwell, K. Lentiviral vector gene therapies come of age with two FDA approvals. *Nature Reviews Drug Discovery* **21**, 790–791 (2022).

[116] Nicolas, C. T. *et al.* In vivo lentiviral vector gene therapy to cure hereditary tyrosinemia type 1 and prevent development of precancerous and cancerous lesions. *Nat Commun* **13**, 5012 (2022).

[117] Laetsch, T. W. *et al.* False-positive results with select HIV-1 NAT methods following lentivirus-based tisagenlecleucel therapy. *Blood* **131**, 2596–2598 (2018).

[118] Banskota, S. *et al.* Engineered virus-like particles for efficient *in vivo* delivery of therapeutic proteins. *Cell* **185**, 250-265.e16 (2022).

[119] Gee, P. *et al.* Extracellular nanovesicles for packaging of CRISPR-Cas9 protein and sgRNA to induce therapeutic exon skipping. *Nat Commun* **11**, 1334 (2020).

[120] Hamilton, J. R. *et al.* In vivo human T cell engineering with enveloped delivery vehicles. *Nat Biotechnol* **42**, 1684–1692 (2024).

[121] Kim, M., Hwang, Y., Lim, S., Jang, H.-K. & Kim, H.-O. Advances in Nanoparticles as Non-Viral Vectors for Efficient Delivery of CRISPR/Cas9. *Pharmaceutics* **16**, 1197 (2024).

[122] Sur, S. *et al.* Recent developments in functionalized polymer nanoparticles for efficient drug delivery system. *Nano-Structures & Nano-Objects* **20**, 100397 (2019).

[123] Ashok, B., Peppas, N. A. & Wechsler, M. E. Lipid- and Polymer-Based Nanoparticle Systems for the Delivery of CRISPR/Cas9. *J Drug Deliv Sci Technol* **65**, 102728 (2021).

[124] Ita, K. Polyplexes for gene and nucleic acid delivery: Progress and bottlenecks. *Eur J Pharm Sci* **150**, 105358 (2020).

[125] Casper, J. *et al.* Polyethylenimine (PEI) in gene therapy: Current status and clinical applications. *Journal of Controlled Release* **362**, 667–691 (2023).

[126] Tenchov, R., Bird, R., Curtze, A. E. & Zhou, Q. Lipid Nanoparticles–From Liposomes to mRNA Vaccine Delivery, a Landscape of Research Diversity and Advancement. *ACS Nano* **15**, 16982–17015 (2021).

[127] Chen, K. *et al.* Lung and liver editing by lipid nanoparticle delivery of a stable CRISPR–Cas9 ribonucleoprotein. *Nat Biotechnol* 1–13 (2024) doi:10.1038/s41587-024-02437-3.

[128] Gillmore, J. D. *et al.* CRISPR-Cas9 In Vivo Gene Editing for Transthyretin Amyloidosis. *New England Journal of Medicine* **385**, 493–502 (2021).

[129] Leal, A. F. *et al.* Iron oxide-coupled CRISPR-nCas9-based genome editing assessment in mucopolysaccharidosis IVA mice. *Mol Ther Methods Clin Dev* **31**, 101153 (2023).

[130] Kaushik, A. *et al.* Magnetically guided non-invasive CRISPR-Cas9/gRNA delivery across blood-brain barrier to eradicate latent HIV-1 infection. *Sci Rep* **9**, 3928 (2019).

[131] Mout, R. & Rotello, V. M. Cytosolic and Nuclear Delivery of CRISPR/Cas9-ribonucleoprotein for Gene Editing Using Arginine Functionalized Gold Nanoparticles. *Bio Protoc* **7**, e2586 (2017).

[132] Shahbazi, R. *et al.* Targeted homology-directed repair in blood stem and progenitor cells with CRISPR nanoformulations. *Nat Mater* **18**, 1124–1132 (2019).

[133] Lewinski, N., Colvin, V. & Drezek, R. Cytotoxicity of Nanoparticles. *Small* **4**, 26–49 (2008).

[134] Turkevich, J., Stevenson, P. C. & Hillier, J. A study of the nucleation and growth processes in the synthesis of colloidal gold. *Discuss. Faraday Soc.* **11**, 55–75 (1951).

[135] Lane, D. D. *et al.* Cas9 RNP Physiochemical Analysis for Enhanced CRISPR-AuNP Assembly and Function. 2024.04.02.586657 Preprint at https://doi.org/10.1101/2024.04.02.586657 (2024).

[136] Danaei, M. *et al.* Impact of Particle Size and Polydispersity Index on the Clinical Applications of Lipidic Nanocarrier Systems. *Pharmaceutics* **10**, 57 (2018).

[137] Zhang, S. & Wang, C. Effect of stirring speed on particle dispersion in silica synthesis. *Nano-Structures & Nano-Objects* **35**, 100994 (2023).

[138] Behzadi, S. *et al.* Cellular Uptake of Nanoparticles: Journey Inside the Cell. *Chem Soc Rev* **46**, 4218–4244 (2017).

[139] Abraham, R. T. & Weiss, A. Jurkat T cells and development of the T-cell receptor signalling paradigm. *Nat Rev Immunol* **4**, 301–308 (2004).

[140] Thongsin, N. & Wattanapanitch, M. CRISPR/Cas9 Ribonucleoprotein Complex-Mediated Efficient B2M Knockout in Human Induced Pluripotent Stem Cells (iPSCs). *Methods Mol Biol* **2454**, 607–624 (2022).

[141] Robbins, P. F. *et al.* Single and dual amino acid substitutions in TCR CDRs can enhance antigen-specific T cell functions. *J Immunol* **180**, 6116–6131 (2008).

[142] Cheng, R. Y.-H. *et al.* Ex vivo engineered human plasma cells exhibit robust protein secretion and long-term engraftment in vivo. *Nat Commun* **13**, 6110 (2022).

[143] Luo, X. M. *et al.* Engineering human hematopoietic stem/progenitor cells to produce a broadly neutralizing anti-HIV antibody after in vitro maturation to human B lymphocytes. *Blood* **113**, 1422–1431 (2009).

[144] Lee, K. *et al.* Nanoparticle delivery of Cas9 ribonucleoprotein and donor DNA in vivo induces homology-directed DNA repair. *Nat Biomed Eng* **1**, 889–901 (2017).

[145] Foss, D. V. *et al.* Peptide-mediated delivery of CRISPR enzymes for the efficient editing of primary human lymphocytes. *Nat. Biomed. Eng* **7**, 647–660 (2023).

[146] Lin, A. Y. et al. Photoablation with the Aurolase System Reduces T Cell Exhaustion and Synergizes with Immunotherapies in Lymphoma. Blood 142, 2825–2825 (2023).

[147] Clark, P. *et al.* Injectable gold for rheumatoid arthritis. *Cochrane Database Syst Rev* **1997**, CD000520 (1997).

[148] Kumthekar, P. *et al.* A first-in-human phase 0 clinical study of RNA interference-based Spherical Nucleic Acids in patients with recurrent Glioblastoma. *Sci Transl Med* **13**, eabb3945 (2021).

[149] Fraietta, J. A. *et al.* Disruption of TET2 promotes the therapeutic efficacy of CD19-targeted T cells. *Nature* **558**, 307–312 (2018).

[150] Krangel, M. S. Mechanics of T cell receptor gene rearrangement. *Curr Opin Immunol* **21**, 133–139 (2009).

[151] Wei, F., Cheng, X.-X., Xue, J. Z. & Xue, S.-A. Emerging Strategies in TCR-Engineered T Cells. *Front. Immunol.* **13**, (2022).

[152] Cohen, C. J. *et al.* Enhanced Antitumor Activity of T Cells Engineered to Express T-Cell Receptors with a Second Disulfide Bond. *Cancer Res* **67**, 3898–3903 (2007).

[153] Rennick, J. J., Johnston, A. P. R. & Parton, R. G. Key principles and methods for studying the endocytosis of biological and nanoparticle therapeutics. *Nat. Nanotechnol.* **16**, 266–276 (2021).

[154] Babu Chandraprabha, P. & Thangavel, S. Endocytosis as a critical regulator of hematopoietic stem cell fate —implications for hematopoietic stem cell and gene therapy. *Stem Cell Research & Therapy* **15**, 319 (2024).

[155] Evnouchidou, I., Caillens, V., Koumantou, D. & Saveanu, L. The role of endocytic trafficking in antigen T cell receptor activation. *Biomed J* **45**, 310–320 (2022).

[156] Panyam, J., Zhou, W.-Z., Prabha, S., Sahoo, S. K. & Labhasetwar, V. Rapid endo-lysosomal escape of poly(DL-lactide-co-glycolide) nanoparticles: implications for drug and gene delivery. *FASEB J* **16**, 1217–1226 (2002).

[157] Karlsson, J., Rhodes, K. R., Green, J. J. & Tzeng, S. Y. Poly(beta-amino ester)s as gene delivery vehicles: challenges and opportunities. *Expert Opin Drug Deliv* **17**, 1395–1410 (2020).

[158] Thasneem, Y. M., Sajeesh, S. & Sharma, C. P. Effect of thiol functionalization on the hemo-compatibility of PLGA nanoparticles. *J Biomed Mater Res A* **99**, 607–617 (2011).

[159] Teo, S. L. Y. *et al.* Unravelling cytosolic delivery of cell penetrating peptides with a quantitative endosomal escape assay. *Nat Commun* **12**, 3721 (2021).

[160] Noel, E. A. *et al.* Hairpin Internal Nuclear Localization Signals in CRISPR-Cas9 Enhance Editing in Primary Human Lymphocytes. *The CRISPR Journal* **8**, 105–119 (2025).

[161] Luk, K. *et al.* Optimization of Nuclear Localization Signal Composition Improves CRISPR-Cas12a Editing Rates in Human Primary Cells. *GEN Biotechnol* **1**, 271–284 (2022).

[162] Moman, R. N., Gupta, N. & Varacallo, M. A. Physiology, Albumin. in *StatPearls* (StatPearls Publishing, Treasure Island (FL), 2025).

[163] Kim, W. *et al.* Protein corona: Friend or foe? Co-opting serum proteins for nanoparticle delivery. *Adv Drug Deliv Rev* **192**, 114635 (2023).

[164] Isolation and functional properties of murine hematopoietic stem cells that are replicating in vivo. *J Exp Med* **183**, 1797–1806 (1996).

[165] Calderbank, E. F., Magnani, L. & Laurenti, E. Intrafemoral Injection of Human Hematopoietic Stem and Progenitor Cells into Immunocompromised Mice. *J Vis Exp* 10.3791/66315 (2023) doi:10.3791/66315